Spatial patterns of temperature, precipitation, and settlement dynamics on the Iberian Peninsula during the Chalcolithic and the Bronze Age

Julien Schirrmacher[1,2], Jutta Kneisel[1,3], Daniel Knitter[1,4], Wolfgang Hamer[1,4], Martin Hinz[1,5], Ralph R. Schneider[1,2,6], Mara Weinelt[1]

[1]CRC 1266, Christian-Albrechts-Universität, Kiel, 24118, Germany

[2]Leibniz-Laboratory for Radiometric Dating and Stable Isotope Research, Christian-Albrechts-Universität, Kiel, 24118, Germany

[3]Institute of Pre- and Protohistoric Archaeology, Christian-Albrechts-Universität, Kiel, 24118, Germany

[4]Department of Geography, Physical Geography, Christian-Albrechts-Universität, Kiel, 24118, Germany

[5]Institute of Archaeology, University of Bern, Bern, 3012, Switzerland

[6]Institute of Geosciences, Christian-Albrechts-Universität, Kiel, 24118, Germany

Corresponding author:

Julien Schirrmacher

jschirrmacher@leibniz.uni-kiel.de

Leibniz-Labor für Altersbestimmung und Isotopenforschung der Christian-Albrechts-Universität zu Kiel

Max-Eyth-Straße 11-13

D-24118 Kiel

Keywords: Iberian Peninsula, temperature, precipitation, Holocene, Chalcolithic, Bronze Age, 4.2 ka BP event, paleoclimatology, data analysis, seasonality

Abstract

In light of recent climate changes, it is important to also gain knowledge about the spatial manifestation of past climate events and their potential impact on ancient societies across a wide range of different scenarios. Following this approach, we compare compilations of seasonal (winter and summer) as well as annual precipitation and temperature changes to a measure of human activity based on AMS ^{14}C data of settlement sites from the Iberian Peninsula during the Chalcolithic and the Bronze Age – a period of major social turnover. Palaeoclimatic reconstructions show a long-term decrease in winter precipitation between 6000 and 3000 cal. BP (4050 – 1050 BCE). Superimposed to this long-term trend in aridification was the 4.2 ka BP climate event, which manifested itself as a period of abrupt decrease in summer precipitation and/or an elongation of the summer dry period, but probably with constant winter precipitation from 4000 to 3800 cal. BP (2050 – 1850 BCE), particularly affecting the southeast of the Iberian Peninsula. Additionally, a winter cooling event across the Iberian Peninsula and its marginal seas occurred between 4400 and 4000 cal. BP (2450 – 2050 BCE) coinciding with Bond Event 3. By comparing human activities to the changes in seasonal and annual precipitation, new insight is gained into the causal relationships between climatic and social dynamics in the past. We show that winter precipitation potentially played a major role for the societies during the Chalcolithic and the Bronze Age of the southern Iberian Peninsula. While the El Argar culture at the south-eastern Iberian Peninsula boomed in spite of enhanced summer drought associated to the 4.2 ka BP climate event, decreasing winter precipitation was potentially contributing to a demographic decline in the southwest after 4800 cal. BP (2850 BCE) as well as to the bust of the El Argar culture in the southeast after 3600 cal. BP (1650 BCE) by limiting the agricultural strategies.

1. Introduction

The current climate change is considered to severely affect people living on the Iberian Peninsula by reducing precipitation and increasing the duration and number of heat waves and dry spells particularly in its Mediterranean region (Giorgi and Lionello, 2008). As a consequence, people likely will increasingly suffer from bad crop yields and bad health status (Kovats et al., 2014). A better understanding of how climate change affected people in the past in marginal environments, which are characterized by large-scale seasonal precipitation and temperature changes, may contribute to the current climate change debate. Such a marginal environment with particular challenges for human societies can be found on the Iberian Peninsula with the spatial and seasonal distribution of precipitation varying considerably. Recently, the south-eastern region, for instance, is the driest area of Europe with an annual average precipitation of less than 400 mm, while the north-western region receives a great amount of annual precipitation (> 1500 mm) (Fick and Hijmans, 2017).

Studying past abrupt climate events in such marginal environments and their potential impact on societies can provide crucial information on the long-term impact of current climate change. In this regard, one of the prime targets for this study is the 4.2 ka BP event, which manifested itself across the Eastern and Central Mediterranean as a prolonged dry episode between 4300 and 3800 cal. BP (calibrated years before present) corresponding to 2350 – 1850 years before the Common Era (BCE) (Cheng et al., 2015; Ruan et al., 2016; Zanchetta et al., 2016). On the Iberian Peninsula a variety of climate records including the 4.2 ka BP event have been published over the last years. These include botanical records in particular, in which discrete climate signals are often masked by variable and highly local land use signals (López-Sáez et al., 2014; Schneider et al., 2016; Fyfe et al., 2019). In this respect, the study of marine archives turns out to be an important tool for regional palaeoclimatic reconstructions as local land use signals are diluted in such archives, which incorporate large-scale regional signals (Faust and Wolf, 2017). Recent studies based on marine archives suggest that the Western Mediterranean area likely experienced stable winter precipitation along with dry summer conditions during the 4.2 ka BP event (Bini et al., 2019; Schirrmacher et al., 2019). Parallel to the precipitation changes, the Western Mediterranean area is also considered by some authors to have experienced a major cooling between 4300 and 3800 cal. BP (2350 – 1850 BCE) (Bini et al., 2019; Català et al., 2019; Zielhofer et al., 2019). However, due to the limited availability of high-resolution and well-dated regional archives, the spatio-temporal manifestation of the 4.2 ka BP event on the Iberian Peninsula remains less clear (Weinelt et al., 2015; Bini et al., 2019).

The climatic deteriorations associated with the 4.2 ka BP event have been shown to have had a large impact on societies in the Near East, where an array of social collapses has been reported along with large-scale population displacements (Welc and Marks, 2014; Weiss, 2017). However, the potential impact of poorly defined climate constraints related to this event on ancient societies of the Iberian Peninsula is still under debate (e.g. Lillios et al., 2016). The rich and well-explored Chalcolithic and Bronze Age archaeological record with many well-dated settlement sites provides a unique archive to explore past social dynamics. Accordingly, an array of studies using summed probability densities (SPDs) of AMS ^{14}C dates as a proxy for human activities and population density in a broader sense have been carried out for the Iberian Peninsula investigating either the role of climate change on societies or the human impact on the environment (Lillios et al., 2016; Drake et al., 2017; Blanco-González et al., 2018; Fyfe et al., 2019; Walsh et al., 2019). Yet, these data are often generalized over a sub-region of the Iberian Peninsula, e.g. the entire Atlantic coast, limiting the detection of the true/full spatial variability within this sub-region. In addition, many studies include data from burial contexts, which likely biases the results towards ritual behaviour (Hinz et al., 2012a). Regarding climatic data, many of the above-mentioned studies just rely on a limited number of single-proxy palaeoclimatic datasets. Considering only a small number of single-proxy data results in potentially large uncertainty questioning their representativeness on a regional scale.

Hence, despite the intense research carried out during the last few years, many crucial questions remain unanswered. These are particularly related to the spatial manifestation of the 4.2 ka BP event on the Iberian Peninsula, which is hampered due to the lack of a coherent data base and the difficult distinction between local anthropogenic and regional climatic signals in many archives. Aiming to address the spatial manifestation of the 4.2 ka BP event on the Iberian Peninsula and trace coherent regional patterns, we compiled a variety of palaeoclimatic proxies from terrestrial and marine archives on the Iberian Peninsula including some sites from northern Africa and its adjacent seas along the Iberian margin, respectively (Fig. 1). Based on this palaeoclimatic multi-proxy compilation, we compare the demographic development of the Iberian Peninsula, which is based on a compilation of AMS^{14}C data from archaeological settlement contexts, with the seasonal (summer and winter) and annual temperature and precipitation history between 6000 and 3000 cal. BP – corresponding to 4050 – 1050 BCE – encompassing the late Neolithic, Chalcolithic and Bronze Age in the area.

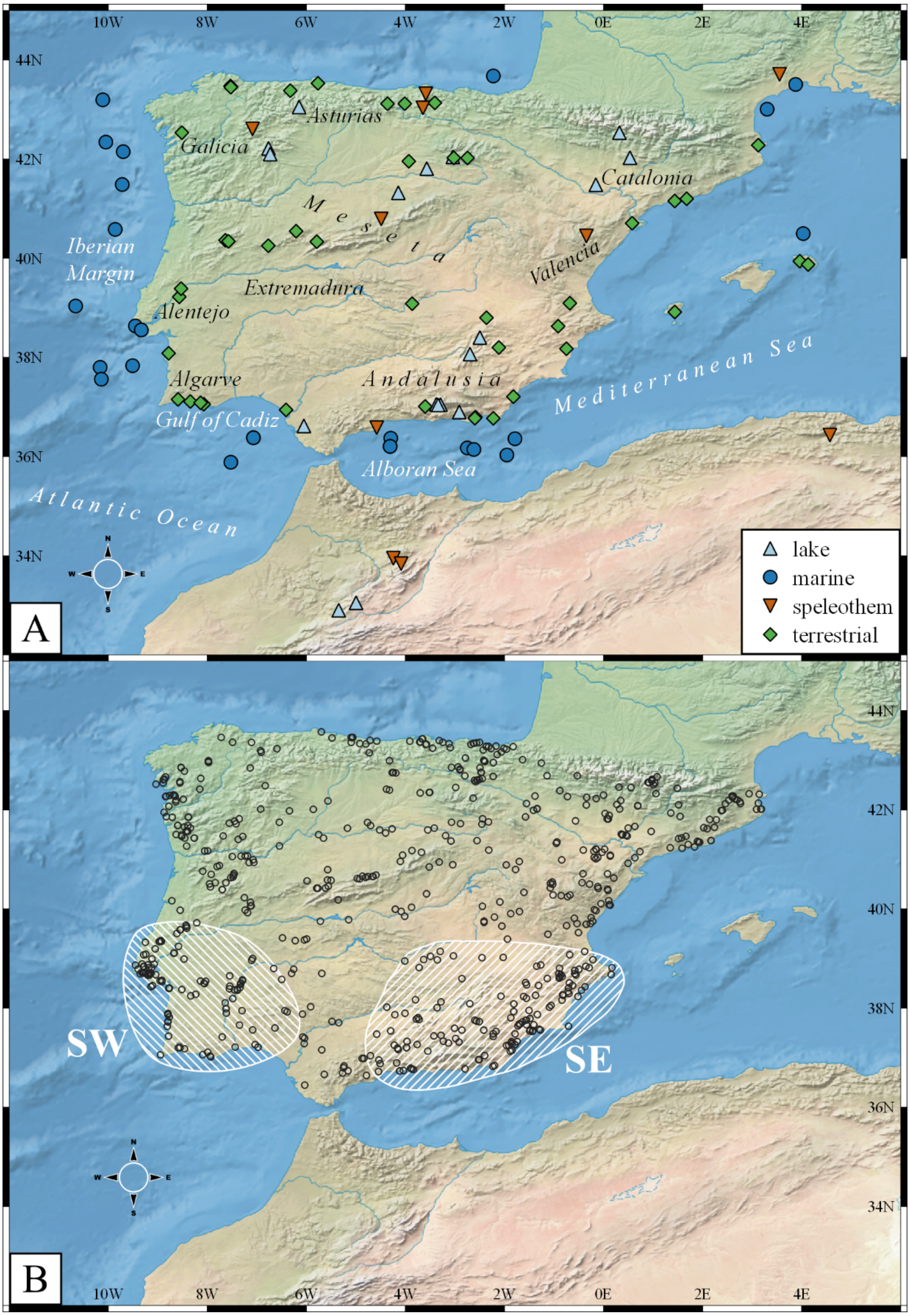

Fig. 1. Overview of the study areas on the Iberian Peninsula and adjacent marine regions showing A) locations of compiled climatic proxies as well as major geographic regions referred to in the text and B) locations of archaeological settlements with AMS ^{14}C dates between 6000 and 3000 cal. BP (4050 – 1050 BCE). Hatched areas indicate geographic regions in the southwest (SW) and the southeast (SE) of similar developments in settlement intensity referred to in the text. For further information on the palaeoclimatic archives see Table 1.

1.1 Climate of the Iberian Peninsula

While during recent times, temperatures across the entire Iberian Peninsula are marked by pronounced seasonal contrasts with more than 20 °C during summer and around 7 °C in winter (Fig. S1; Fick and Hijmans, 2017), the distribution of precipitation reveals a marked regional pattern, which is mainly driven by the Atlantic and Mediterranean atmospheric regimes (Lionello, 2012). Today, precipitation on the Iberian Peninsula in general is associated with the westerly wind belt (Zorita et al., 1992) and to a large extent controlled by the North Atlantic Oscillation (Hurrell, 1995; Trigo et al., 2004; Hernández et al., 2015). However, the Atlantic climate is bounded to the northern and western coasts and typically marked by high precipitation of 400 mm to more than 1000 mm during the rainy season from October to February and between 300 mm and 700 mm from March to September (Fig. S1; Fick and Hijmans, 2017). In contrast, the Mediterranean climate, which is most pronounced at the southern and eastern coasts as well as in the Meseta area, is characterized by significantly drier conditions with a rainy winter season (up to 500 mm) and a dry summer season barely exceeding 200 mm (Fig. S1; Fick and Hijmans, 2017).

Given that the variability of sea surface temperatures (SSTs) and atmospheric temperatures at Iberian coasts are tightly coupled (Fig. S2), the marine conditions with respect to temperature, in particular, are of major importance for the climate system across the Iberian Peninsula. Regarding the SSTs, a strong seasonal contrast is evident at the western coast, which receives warm waters with the Iberian Poleward Current from the south during the winter season (Peliz et al., 2005). During the summer, however, the surface current is directed southward and favours coastal upwelling along the western continental margin, thus, causing relatively low SSTs (Haynes et al., 1993; Peliz et al., 2002). At the southern coast in the Alboran Sea Atlantic water masses circulate in two anti-cyclonic gyres (Lionello, 2012). These gyres promote local upwelling and, thus, also modulate the regional temperature variability in the Alboran Sea (Sarhan et al., 2000).

Over the course of the Holocene, climatic conditions on the Iberian Peninsula and adjacent marine areas were modulated by long-term trends as well as by superimposed abrupt events. In relation to decreasing solar forcing from the beginning of the Holocene, the Iberian Peninsula faced a trend towards cooler and drier conditions (Cacho et al., 2001; Peyron et al., 2017; Ramos-Román et al., 2018). The overall cooling trend is questioned by (Davis et al., 2003), though, who based on pollen data found a warming trend since ca. 8000 cal. BP (6050 BCE) across south-west Europe. Nonetheless, the Holocene Climatic Optimum between ca. 9500 and 7600 cal. BP (7550 – 5650 BCE) is associated with maximum extension of the forest cover at the Iberian Peninsula suggesting intense winter precipitation and high temperatures (Jalut et al., 2009; Ramos-Román et al., 2018). Afterwards, a trend towards increasing aridity is particularly evident since around 5500 cal. BP (3550 BCE) (Jalut et al., 2009; Jiménez-Moreno et al., 2015). Also, between 7000 and 5000 cal. BP (5050 – 3050 BCE) the Mediterranean climate characterized by mild winters as well as hot and dry summers gradually established on the Iberian Peninsula (Pérez-Obiol et al., 2011). Seasonality in sea surface temperatures, on the other hand, became smaller, i.e. cooler summers and warmer winters, during the Holocene, which is particularly evident in the Atlantic realm (Schirrmacher et al., 2019). These long-term trends are amplified by several dry and cool episodes (Cacho et al., 2001; Chabaud et al., 2014; Ramos-Román et al., 2018; Schirrmacher et al., 2019; Zielhofer et al., 2019). These dry and cool episodes are modulated by the interference of North Atlantic (subpolar) and Mediterranean (subtropical) climatic regimes. For instance, the North Atlantic Oscillation controlled winter precipitation variability on the Iberian Peninsula since the mid-Holocene (Ausín et al., 2015; Wassenburg et al., 2016; Zielhofer et al., 2017; Schirrmacher et al., 2019). Holocene cooling events on the Iberian Peninsula, on the other hand, were related to the so-called Bond Events (Bond et al., 2001), a series of iceberg discharge events in the North Atlantic (Smith et al., 2016; Ramos-Román et al., 2018; Schirrmacher et al., 2019; Zielhofer et al., 2019).

1.2 Archaeological background

Detailed reviews of the prehistoric developments on the Iberian Peninsula are beyond the scope of this study and can be found elsewhere (Chapman, 2008; Lull et al., 2013a; Blanco-González et al., 2018). The following summary intends to provide an overview of the most important cultural developments during the Chalcolithic (c. 5300 – 4200 cal. BP; 3300 – 2200 BCE) and Bronze Age (c. 4200 – 2900 cal. BP; 2200 – 900 BCE).

The Chalcolithic or Copper Age marks the beginning of metallurgy, namely copper metalworking (Bartelheim and Pearce, 2015). Whereas people in Galicia, Asturias, and the northern Meseta mainly lived in small farmsteads (Blanco-González et al., 2018), in the southern part of the Iberian Peninsula in Alentejo and Andalusia people nucleated and major sites such as Zambujal and Los Millares emerged (Molina González et al., 2004; Kunst and Lutz, 2008). As suggested from different trade networks (Schuhmacher, 2017), both sites likely reflect two distinct social systems: a society close to the site of Zambujal in the southwest (SW) at the Atlantic coast and the Los Millares culture in the southeast (SE) at the Mediterranean coast. Furthermore, defensive structures associated with many sites and specialized manufacture of arrowheads in both regions indicate that violent conflicts were prominent features between rivalling societies at that time (Lull et al., 2015). Apart from these notable differences, both societies share numerous similarities, for example, the use of Bell Beaker pottery (Müller and van Willigen, 2001), a megalithic burial tradition (Schulz Paulsson, 2019), or participation in long-distance exchange networks (Schuhmacher, 2017). Moreover, settlement sites share similarities with the occurrence of major sites including ditched and walled enclosures (sometimes on hilltops), or pit complexes (Lull et al., 2015; Valera, 2015; Blanco-González et al., 2018), which are perhaps the most prominent and best explored settlement features from that time. So-called mega-sites, for instance, Valencina de la Concepción or Marroquíes Bajos encompassed an area of up to 450 and 113 hectares, respectively (García Sanjuán et al., 2017). Apart from these, also small sites in the lowlands associated with increased agricultural production, whose frequencies are likely underestimated due to their low visibility in the field, were settled in the south at that time (Chapman, 2008; García Sanjuán et al., 2016).

The period around c. 4200 cal. BP (2250 BCE) marks a time of major societal turnover and transformation on the Iberian Peninsula, particularly in the south spanning economic, ritual, and traditional practises as well as settlement patterns. In the SW, including the Alentejo and Algarve regions, the majority of sites – also those with ditched enclosures and large walled sites – were abandoned and also many traditions (e.g. material culture and burial customs) vanished (Soares et al., 2007; Lull et al., 2015; Valera, 2015). The rapidity of these transformations, which occurred within some decades (Lull et al., 2015; García Sanjuán et al., 2018), imply a social collapse in the area. Subsequently, a semi-nomadic lifestyle was established in the Alentejo, Algarve, and Extremadura regions (Lull et al., 2013a; Valera, 2015). In the Meseta, agricultural activity sharply dropped between 4200 and 4000 cal. BP (2250 – 2050 BCE) and people increasingly relied on pastoralism (López Saez et al., 2017). Furthermore, the site of Los Millares in Andalusia decreased significantly between 4500 and 4200 cal. BP (2550 – 2250 BCE) and probably ended violently by fire (Lull et al., 2015).

In the beginning of the Bronze Age, bronze and later silver metallurgy were introduced to the Iberian Peninsula (Comendador Rey et al., 2014). Nonetheless, in Galicia and Asturias social developments are considered to be marked by relative stability in terms of subsistence strategies (i.e. small number of lowland sites mainly dependent on agriculture). Andalusia and the southern parts of the Meseta and Valencia, in contrast, featured the rise of the El Argar civilization, which is regarded as the first political and hierarchical society on the Iberian Peninsula with broad control of specialized metallurgy and agricultural practises (Lull et al., 2011; Delgado-Raack et al., 2014; Delgado-Raack and Risch, 2015). Based on differential endowments of grave goods, Lull et al. (2011) have defined five to six distinct social classes underlining the hierarchical system of the Argaric culture. The Argaric culture spread from the south eastern coast along the Valencian coast and extended into the southern Meseta within about 300 years and is also associated with a demographic boom in these areas (Aranda et al., 2008; Chapman, 2008; Lull et al., 2011). Prominent settlement types were hilltop sites in the mountains (Chapman, 2008) and fortified settlements (*motillas*) in the upper Guadalquivir and Guadiana river basins (Aranda et al., 2008). The *motillas* were used for groundwater extraction supplying the intense agriculture practised at that time (Benítez de Lugo Enrich and Mejías, 2017). Overall, irrigation techniques were known in the Argaric culture and spread westwards during the following centuries (Mora-González et al., 2016; Mora-González et al., 2018). While the Argaric people were not engaged in trans-regional trade, highly specialized manufacturing processes are documented (Delgado-Raack and Risch, 2015). Starting from the hilltop settlements, where the elites and, thus, the political power was situated, intense agricultural production took place in the lowlands (Castro et al., 1999; Aranda et al., 2008). Processing of cereals took place in specialized workshops at the hilltop sites, while the food was stored in different areas within the sites where it was redistributed by the elites (Delgado-Raack and Risch, 2015). It has been proposed that the end of the Argaric culture by c. 3500 cal. BP (1550 BCE) is characterized by environmental over-exploitation due to intense agriculture (Chapman, 2008). At that time, 50 to 100 per cent of Argaric settlements, among them hilltop sites and the *motillas*, were abandoned and replaced by small sites based on subsistence (Lull et al., 2013a). Along with the collapse of the Argaric culture, its political system also disappeared (Chapman, 2008).

2. Methods

2.1 Palaeoclimatological compilation and approach

In this paper, we compiled climate data from various archives (Fig. 1) including multiple proxies to limit potential biases from single-proxy approaches and to identify coherent regional climatic patterns on the Iberian Peninsula. Temperature and precipitation compilations based on own data (Schirrmacher et al., 2019) and other published data have been accomplished from various databases such as SISAL (Atsawawaranunt et al., 2019), PANGAEA WDC-Mare, NOAA, and European Pollen Database (Table 1). Temperature and precipitation have been chosen as main climatic variables confining agricultural activities and abrupt changes of those variables are considered as hazardous, and thus, as crucial for the subsistence/ economies of ancient societies. The database compiled for this study contains 157 datasets from 95 sites between 12°W and 6°E and 32°N to 45°N (Fig. 1; Table 1). Altogether, the database comprises records from 18 lake archives, 25 marine sites, 10 speleothems, and 42 other terrestrial archives (e.g. peat deposits), and is based on 18 different quantitative or qualitative proxies. While 111 datasets reflect precipitation changes, 46 datasets are indicative of sea surface and/or atmospheric temperature variability. With 97 datasets pollen represent the majority of the compiled proxies.

The compiled temperature data from marine sediment archives are based on a suite of biomarker and other semi-quantitative and quantitative proxies that enable to assess the variability of precipitation and temperature at seasonal or annual scale. These include long-chain diol indexes (LDI), alkenones, TEX86, and planktonic foraminiferal assemblages transferred to temperatures via modern analogue technique (MAT), all reflecting sea surface temperatures (SSTs). A tight coupling between SST and atmospheric temperature variability along the Iberian coasts is suggested from observational data (Fig. S2) and justifies the use of SST data for a comparative study with archaeological data. To assess seasonality as a variable potentially highly influential to agrarian production, the compiled climatic proxy data were assigned to individual seasons wherever possible. Following Gouveia et al. (2008), we considered decreasing arboreal pollen (AP) percentages on the Iberian Peninsula as reflecting a decrease in winter precipitation. This is in harmony with interpretations in previous palaeoclimatic studies from the Iberian Peninsula (Fletcher et al., 2010; Chabaud et al., 2014; Ramos-Román et al., 2018). Contrastingly, xerophytic species such as Chenopodiaceae, Amaranthaceae, and

Table 1

Palaeoclimatic proxies compiled for this study. [a] The age model for this archive has been re-calculated for this study. The individual age-depth models are shown in Fig. S3. [b] The data has been digitized from the original reference. The assignment of the final quality flag (QF) based on the number of datings, the temporal coverage, and the average temporal resolution is explained in Table 2. Parameter-based QFs for number of datings, temporal coverage, and temporal resolution are shown in brackets. preWin = 2000 – 3000 cal. BP (50 – 1050 BCE); Win = 3000 – 6000 cal. BP (1050 – 4050 BCE); postWin = 6000 – 7000 cal. BP (4050 – 5050 BCE)

Name	Latitude	Longitude	Archive	Proxy	No. of datings preWin/Win/postWin (parameter-based QF)	Temporal coverage in Win (parameter-based QF)	Temporal resolution (parameter-based QF)	Final QF	References
Precipitation									
annual									
Monte Areo	43.528889	-5.768889	terrestrial	pollen WAPLS	1/1/2 (2)	85 % (1)	427 yrs (3)	3	(Ilvonen et al., in review)
PB06	43.506604	3.875170	marine	XRD data	6/7/2 (1)	99 % (1)	20 yrs (1)	1	(Sabatier et al., 2012)
Alto de la Espina	43.381111	-6.327222	terrestrial	pollen WAPLS	2/3/0 (1)	95 % (1)	178 yrs (2)	2	(Ilvonen et al., in review)
Zalama	43.135000	-3.409722	terrestrial	pollen WAPLS	0/6/3 (1)	97 % (1)	72 yrs (1)	1	(Ilvonen et al., in review)
Alsa	43.117778	-4.016667	terrestrial	Chenopodiaceae	1/1/0 (2)	40 % (3)	101 yrs (2)	3	(Mariscal, 1993)
Lago de Ajo[a,b]	43.050000	-6.150000	lake	pollen MAT	0/1/0 (3)	94 % (1)	201 yrs (3)	3	(Allen et al., 1996)
KGSC-31[b]	43.006389	3.298889	marine	n-alkane concentration	1/4/2 (1)	99 % (1)	15 yrs (1)	1	(Jalali et al., 2016)
Basa de la Mora[b]	42.533333	0.316667	lake	*Artemisia*	2/3/1 (1)	100 % (1)	125 yrs (2)	2	(Pérez-Sanz et al., 2013)
Laguna de la Roya[a,b]	42.216667	-6.766667	lake	pollen MAT	0/1/1 (2)	90 % (1)	209 yrs (3)	3	(Allen et al., 1996)
Sanabria[a,b]	42.100000	-6.733333	lake	pollen MAT	0/0/0 (3)	94 % (1)	177 yrs (2)	3	(Allen et al., 1996)
Las Pardillas	42.045556	-3.045278	lake	Xerophytes	0/1/0 (3)	86 % (1)	184 yrs (2)	3	(Sánchez Goñi and Hannon, 1999)
Estanya	42.027139	0.5304340	lake	PCA2 XRF data	0/1/2 (2)	93 % (1)	15 yrs (1)	2	(Morellón et al., 2009)
Quintanar de la Sierra	42.025278	-3.026111	terrestrial	pollen WAPLS	0/1/0 (3)	69 % (2)	347 yrs (3)	3	(Ilvonen et al., in review)
Espinosa de Cerrato[b]	41.956667	-3.935000	terrestrial	*Artemisia*	1/2/0 (2)	99 % (1)	68 yrs (1)	2	(Franco-Múgica et al., 2001)
Hoya del Castillo	41.481944	-0.158333	lake	Xerophytes	0/0/1 (3)	44 % (3)	187 yrs (2)	3	(Davis and Stevenson, 2007)
Amposta[b]	40.706669	0.574036	terrestrial	*Artemisia*	1/3/0 (2)	90 % (1)	208 yrs (3)	3	(Pérez-Obiol et al., 2011)
El Maíllo	40.546667	-6.209722	terrestrial	pollen WAPLS	0/2/0 (2)	95 % (1)	130 yrs (2)	2	(Ilvonen et al., in review)
MD99-2343	40.497333	4.028167	marine	potassium/ aluminium ratio	1/1/2 (2)	98 % (1)	140 yrs (2)	2	(Frigola et al., 2008)
Algendar	39.940556	3.958611	terrestrial	Xerophytes	0/2/1 (2)	99 % (1)	65 yrs (1)	2	(Yll et al., 1997)
Hort Timoner	39.875000	4.126389	terrestrial	Xerophytes	0/0/0 (3)	98 % (1)	118 yrs (2)	3	(Yll et al., 1997)
Navarrés	39.093333	-0.683333	terrestrial	pollen WAPLS	0/1/1 (2)	98 % (1)	113 yrs (2)	2	(Ilvonen et al., in review)
MD03-2699	39.036700	-10.660500	marine	n-alkane concentration	0/2/0 (2)	92 % (1)	154 yrs (2)	2	(Palumbo et al., 2013)
Villaverde[b]	38.800000	-2.366667	terrestrial	Xerophytes	2/2/0 (2)	96 % (1)	57 yrs (1)	2	(Carrión et al., 2001a)
D13882	38.634500	-9.454200	marine	n-alkane concentration	1/1/1 (2)	97 % (1)	112 yrs (2)	2	(Rodrigues et al., 2009)
D13902	38.554000	-9.335500	marine	n-alcohol concentation	0/0/1 (3)	36 % (3)	271 yrs (3)	3	(Rodrigues et al., 2009)
Siles[b]	38.400000	-2.500000	lake	Xerophytes	1/3/0 (2)	97 % (1)	162 yrs (2)	2	(Carrión, 2002)
El Sabinar[a,b]	38.200000	-2.116667	terrestrial	Xerophytes	2/4/1 (1)	97 % (1)	81 yrs (1)	1	(Carrión et al., 2004)
Elx	38.174444	-0.752778	terrestrial	Xerophytes	0/2/1 (2)	75 % (2)	45 yrs (1)	2	(Burjachs et al., 1997)
Santo Andre[a,b]	38.083333	-8.783333	terrestrial	Chenopodiaceae	0/2/1 (2)	74 % (2)	369 yrs (3)	3	(Santos and Sánchez Goñi, 2003)
Cañada de la Cruz[a,b]	38.066667	-2.700000	lake	Xerophytes	3/3/1 (1)	96 % (1)	206 yrs (3)	3	(Carrión et al., 2001b)
MD95-2042[b]	37.799833	-10.166500	marine	Chenopodiaceae	1/2/1 (2)	90 % (1)	180 yrs (2)	2	(Chabaud et al., 2014)
Antas	37.208333	-1.823611	terrestrial	Xerophytes	0/0/0 (3)	86 % (1)	369 yrs (3)	3	(Pantaléon-Cano et al., 2003)
P01-5[b]	37.085105	-8.138509	terrestrial	*Artemisia*	4/4/0 (1)	68 % (2)	156 yrs (2)	2	(Schneider et al., 2010; Schneider et al., 2016)

Name	Latitude	Longitude	Archive	Proxy	No. of datings preWin/Win/postWin (parameter-based QF)	Temporal coverage in Win (parameter-based QF)	Temporal resolution (parameter-based QF)	Final QF	References
Borreguil de la Virgen[b]	37.054167	-3.377778	lake	*Artemisia*	0/3/1 (2)	95 % (1)	72 yrs (1)	2	(Jiménez-Moreno and Anderson, 2012)
Laguna Hondera[b]	37.048000	-3.294333	lake	calcium/titanium ratio	1/1/2 (2)	94 % (1)	118 yrs (2)	2	(Mesa-Fernández et al., 2018)
Laguna de Río Seco[b]	37.040500	-3.342833	lake	*Artemisia*	1/3/2 (1)	97 % (1)	139 yrs (2)	2	(Anderson et al., 2011)
Padul[b]	37.011047	-3.603906	terrestrial	Xerophytes	2/4/2 (1)	98 % (1)	55 yrs (1)	1	(Ramos-Román et al., 2018)
Donana[b]	36.941667	-6.413333	terrestrial	Amaranthaceae	1/4/0 (1)	68 % (2)	120 yrs (2)	2	(Jiménez-Moreno et al., 2015)
Sierra de Gádor[a,b]	36.900000	-2.916667	lake	Xerophytes	0/1/2 (2)	98 % (1)	65 yrs (1)	2	(Carrión et al., 2003)
Roquetas de Mar	36.794444	-2.588889	terrestrial	Xerophytes	0/1/1 (2)	97 % (1)	162 yrs (2)	2	(Pantaléon-Cano et al., 2003)
San Rafael	36.773611	-2.601389	terrestrial	Xerophytes	0/1/0 (3)	86 % (1)	90 yrs (1)	3	(Pantaléon-Cano et al., 2003)
San Rafael	36.773611	-2.601389	terrestrial	pollen WAPLS	0/1/0 (3)	86 % (1)	90 yrs (1)	3	(Ilvonen et al., in review)
Lake Medina[b]	36.617778	-6.053611	lake	ostracod assemblages	3/5/3 (1)	99 % (1)	74 yrs (1)	1	(Schröder et al., 2018)
El Refugio Cave	36.583333	-4.583333	speleothem	CT density	0/6/0 (1)	100 % (1)	3 yrs (1)	1	(Walczak et al., 2015)
Gueldaman Cave	36.433300	4.566700	speleothem	stalagmite $\delta^{18}O$	0/8/0 (1)	87 % (1)	13 yrs (1)	1	(Ruan et al., 2016)
TTR14-300G[b]	36.358867	-1.791783	marine	lanthanum/ lutetium ratio	0/0/1 (3)	90 % (1)	244 yrs (3)	3	(Cortés-Sánchez et al., 2011)
ODP-161-976A[a,b]	36.205333	-4.312667	marine	pollen MAT	0/11/0 (1)	86 % (1)	259 yrs (3)	3	(Combourieu Nebout et al., 2009)
MD95-2043	36.143333	-2.621167	marine	pollen MAT	0/2/1 (2)	94 % (1)	117 yrs (2)	2	(Bini et al., 2019); (Fletcher et al., 2010); (Peyron et al., 2017)
MD95-2043	36.143333	-2.621167	marine	Xerophytes	0/2/1 (2)	94 % (1)	117 yrs (2)	2	(Fletcher and Sánchez Goñi, 2008)
summer									
ODP-161-976A[a,b]	36.205333	-4.312667	marine	pollen MAT	0/11/0 (1)	86 % (1)	259 yrs (3)	3	(Combourieu Nebout et al., 2009)
MD95-2043	36.143334	-2.621168	marine	pollen MAT	0/2/1 (2)	94 % (1)	117 yrs (2)	2	(Bini et al., 2019); (Fletcher et al., 2010); (Peyron et al., 2017)
winter									
Cuadramón	43.474167	-7.534722	terrestrial	arboreal pollen	0/0/0 (3)	74 % (2)	442 yrs (3)	3	(González and Saa, 2000)
Pedrido	43.450278	-7.529167	terrestrial	arboreal pollen	8/9/0 (1)	76 % (2)	79 yrs (1)	2	(Stefanini et al., 2018)
Cueva de Asiul	43.316842	-3.591200	speleothem	stalagmite $\delta^{18}O$	2/3/1 (1)	100 % (1)	15 yrs (1)	1	(Smith et al., 2016)
Alsa	43.117778	-4.016667	terrestrial	arboreal pollen	1/1/0 (2)	40 % (3)	101 yrs (2)	3	(Mariscal, 1993)
Avellanosa	43.116667	-4.364167	terrestrial	arboreal pollen	1/0/1 (2)	92 % (1)	184 yrs (2)	2	(Mariscal, 1983)
Cova da Arcoia	42.610000	-7.090000	speleothem	stalagmite $\delta^{13}C$	1/7/1 (1)	89 % (1)	65 yrs (1)	1	(Railsback et al., 2011)
Basa de la Mora[b]	42.533333	0.316667	lake	arboreal pollen	2/3/1 (1)	100 % (1)	125 yrs (2)	2	(Pérez-Sanz et al., 2013)
PRD-4	42.533333	-8.516667	terrestrial	arboreal pollen	0/2/1 (2)	91 % (1)	248 yrs (3)	3	(López-Merino et al., 2012)
Castelló d'Empúries[b]	42.281389	3.120278	terrestrial	arboreal pollen	1/0/1 (2)	96 % (1)	240 yrs (3)	3	(Burjachs and Expósito, 2015)
Las Pardillas	42.045556	-3.045278	lake	arboreal pollen	0/1/0 (3)	86 % (1)	184 yrs (2)	3	(Sánchez Goñi and Hannon, 1999)
Hoyos de Iregua[a,b]	42.023889	-2.750000	terrestrial	arboreal pollen	0/0/1 (3)	94 % (1)	257 yrs (3)	3	(Gil García et al., 2002)
Espinosa de Cerrato[b]	41.956667	-3.935000	terrestrial	arboreal pollen	1/2/0 (2)	99 % (1)	68 yrs (1)	2	(Franco-Múgica et al., 2001)
Tubilla del Lago	41.808417	-3.572675	lake	arboreal pollen	1/4/2 (1)	99 % (1)	80 yrs (1)	1	(Morales-Molino et al., 2017)
Hoya del Castillo	41.481944	-0.158333	lake	arboreal pollen	0/0/1 (3)	44 % (3)	187 yrs (2)	3	(Davis and Stevenson, 2007)
El Carrizal[a,b]	41.320028	-4.146972	lake	arboreal pollen	0/1/0 (3)	91 % (1)	227 yrs (3)	3	(Franco-Múgica et al., 2005)
Cubelles[b]	41.200278	1.675000	terrestrial	arboreal pollen	1/1/0 (2)	95 % (1)	167 yrs (2)	2	(Burjachs and Expósito, 2015)
Creixell[b]	41.155556	1.433889	terrestrial	arboreal pollen	0/1/1 (2)	89 % (1)	223 yrs (3)	3	(Burjachs and Expósito, 2015)
Molinos Cave	40.792500	-4.492000	speleothem	stalagmite $\delta^{13}C$	1/3/1 (1)	90 % (1)	31 yrs (1)	1	(Muñoz et al., 2015)
Amposta[b]	40.706669	0.574036	terrestrial	arboreal pollen	1/3/0 (2)	90 % (1)	208 yrs (3)	3	(Pérez-Obiol et al., 2011)

Name	Latitude	Longitude	Archive	Proxy	No. of datings preWin/Win/postWin (parameter-based QF)	Temporal coverage in Win (parameter-based QF)	Temporal resolution (parameter-based QF)	Final QF	References
El Maíllo	40.546667	-6.209722	terrestrial	arboreal pollen	0/2/0 (2)	89 % (1)	121 yrs (2)	2	(Morales-Molino et al., 2013)
Ejulve Cave	40.450000	-0.350000	speleothem	stalagmite $\delta^{13}C$	4/15/2 (1)	100 % (1)	13 yrs (1)	1	(Moreno et al., 2017)
Lagoa Comprida[a]	40.362778	-7.636111	terrestrial	arboreal pollen	0/2/0 (2)	93 % (1)	117 yrs (2)	2	(van den Brink and Janssen, 1985)
Charco de Candieira[a]	40.341667	-7.576389	terrestrial	arboreal pollen	3/5/2 (1)	97 % (1)	56 yrs (1)	1	(van der Knaap and van Leeuwen, 1995)
Peña Negra	40.334722	-5.792222	terrestrial	arboreal pollen	1/1/0 (2)	34 % (3)	92 yrs (1)	3	(Abel-Schaad and López-Sáez, 2013)
El Payo	40.253333	-6.771111	terrestrial	arboreal pollen	0/1/0 (3)	25 % (3)	150 yrs (2)	3	(Abel Schaad et al., 2009)
Algendar	39.940556	3.958611	terrestrial	arboreal pollen	0/2/1 (2)	99 % (1)	65 yrs (1)	2	(Yll et al., 1997)
Hort Timoner	39.875000	4.126389	terrestrial	arboreal pollen	0/0/0 (3)	98 % (1)	118 yrs (2)	3	(Yll et al., 1997)
0501.029[b]	39.387519	-8.532257	terrestrial	arboreal pollen	1/2/2 (2)	94 % (1)	202 yrs (3)	3	(Vis et al., 2010)
ALP III[b]	39.221083	-8.568478	terrestrial	arboreal pollen	1/1/2 (2)	96 % (1)	80 yrs (1)	2	(Vis et al., 2010)
CC-17[a,b]	39.083333	-3.866667	terrestrial	arboreal pollen	0/0/0 (3)	91 % (1)	228 yrs (3)	3	(Dorado Valiño et al., 2002)
Eivissa[b]	38.915833	1.435000	terrestrial	arboreal pollen	1/2/0 (2)	89 % (1)	178 yrs (2)	2	(Burjachs and Expósito, 2015)
Villaverde[b]	38.800000	-2.366667	terrestrial	arboreal pollen	2/2/0 (2)	96 % (1)	57 yrs (1)	2	(Carrión et al., 2001a)
Villena[a,b]	38.629667	-0.919889	terrestrial	aridity ratio	0/3/0 (2)	83 % (1)	146 yrs (2)	2	(Jones et al., 2018)
Elx	38.174444	-0.752778	terrestrial	arboreal pollen	0/2/1 (2)	75 % (2)	45 yrs (1)	2	(Burjachs et al., 1997)
Santo Andre[a,b]	38.083333	-8.783333	terrestrial	arboreal pollen	0/2/1 (2)	74 % (2)	369 yrs (3)	3	(Santos and Sánchez Goñi, 2003)
Cañada de la Cruz[a,b]	38.066667	-2.700000	lake	arboreal pollen	3/3/1 (1)	96 % (1)	206 yrs (3)	3	(Carrión et al., 2001b)
MD95-2042[b]	37.799833	-10.166500	marine	arboreal pollen	1/2/1 (2)	90 % (1)	180 yrs (2)	2	(Chabaud et al., 2014)
Antas	37.208333	-1.823611	terrestrial	arboreal pollen	0/0/0 (3)	86 % (1)	369 yrs (3)	3	(Pantaléon-Cano et al., 2003)
ABI 05/07[b]	37.152416	-8.594227	terrestrial	arboreal pollen	1/6/1 (1)	97 % (1)	121 yrs (2)	2	(Trog et al., 2013; Schneider et al., 2016)
ADP 01/06[b]	37.110503	-8.345146	terrestrial	arboreal pollen	1/2/0 (2)	98 % (1)	419 yrs (3)	3	(Trog et al., 2013); (Schneider et al., 2016)
P01-5[b]	37.085105	-8.138509	terrestrial	arboreal pollen	4/4/0 (1)	68 % (2)	156 yrs (2)	2	(Schneider et al., 2010; Schneider et al., 2016)
VDL PB2[b]	37.055965	-8.074490	terrestrial	arboreal pollen	3/1/3 (2)	16 % (3)	32 yrs (1)	3	(Schneider et al., 2010; Schneider et al., 2016)
Borreguil de la Virgen[b]	37.054167	-3.377778	lake	arboreal pollen	0/3/1 (2)	95 % (1)	72 yrs (1)	2	(Jiménez-Moreno and Anderson, 2012)
Laguna de Río Seco[b]	37.040500	-3.342833	lake	arboreal pollen	1/3/2 (1)	97 % (1)	139 yrs (2)	2	(Anderson et al., 2011)
Padul[b]	37.011047	-3.603906	terrestrial	arboreal pollen	2/4/2 (1)	98 % (1)	55 yrs (1)	1	(Ramos-Román et al., 2018)
Donana[b]	36.941667	-6.413333	terrestrial	arboreal pollen	1/4/0 (1)	68 % (2)	120 yrs (2)	2	(Jiménez-Moreno et al., 2015)
Sierra de Gádor[a,b]	36.900000	-2.916667	lake	arboreal pollen	0/1/2 (2)	98 % (1)	65 yrs (1)	2	(Carrión et al., 2003)
Roquetas de Mar	36.794444	-2.588889	terrestrial	arboreal pollen	0/1/1 (2)	97 % (1)	162 yrs (2)	2	(Pantaléon-Cano et al., 2003)
San Rafael	36.773611	-2.601389	terrestrial	arboreal pollen	0/1/0 (3)	86 % (1)	90 yrs (1)	3	(Pantaléon-Cano et al., 2003)
Cabo de Gata[b]	36.771389	-2.228611	terrestrial	arboreal pollen	0/1/1 (2)	97 % (1)	103 yrs (2)	2	(Burjachs and Expósito, 2015)
GeoB5901-2[a]	36.380000	-7.071333	marine	n-alkane concentration	3/12/1 (1)	78 % (2)	69 yrs (1)	2	(Schirrmacher et al., 2019)
ODP-161-976A[a]	36.205333	-4.312667	marine	n-alkane concentration	0/11/0 (1)	91 % (1)	29 yrs (1)	1	(Schirrmacher et al., 2019)
ODP-161-976A[a,b]	36.205333	-4.312667	marine	pollen MAT	0/11/0 (1)	86 % (1)	259 yrs (3)	3	(Combourieu Nebout et al., 2009)
MD95-2043	36.143333	-2.621167	marine	pollen MAT	0/2/1 (2)	94 % (1)	117 yrs (2)	2	(Bini et al., 2019); (Fletcher et al., 2010); (Peyron et al., 2017)
MD95-2043	36.143333	-2.621167	marine	arboreal pollen	0/2/1 (2)	94 % (1)	117 yrs (2)	2	(Fletcher and Sánchez Goñi, 2008)

Name	Latitude	Longitude	Archive	Proxy	No. of datings preWin/Win/postWin (parameter-based QF)	Temporal coverage in Win (parameter-based QF)	Temporal resolution (parameter-based QF)	Final QF	References
Chaara Cave 1	33.950000	-4.246000	speleothem	stalagmite $\delta^{18}O$	3/6/4 (1)	100 % (1)	9 yrs (1)	1	(Ait Brahim et al., 2019)
Chaara Cave 2	33.950000	-4.246000	speleothem	stalagmite $\delta^{18}O$	3/10/3 (1)	98 % (1)	12 yrs (1)	1	(Ait Brahim et al., 2019)
Grotte de Piste	33.840000	-4.090000	speleothem	stalagmite $\delta^{18}O$	1/6/4 (1)	99 % (1)	14 yrs (1)	1	(Wassenburg et al., 2016)
Lake Sidi Ali	33.050000	-5.000000	lake	ostracod $\delta^{18}O$	2/5/1 (1)	98 % (1)	89 yrs (1)	1	(Zielhofer et al., 2019)
Tigalmamine[b]	32.900000	-5.350000	lake	shallow water diatom-species	1/1/0 (2)	96 % (1)	107 yrs (2)	2	(Lamb and van der Kaars, 1995)
				Temperature					
annual									
Grotte de Clamouse	43.710000	3.550000	speleothem	stalagmite $\delta^{18}O$	2/2/0 (2)	99 % (1)	47 yrs (1)	2	(McDermott et al., 1999)
PP10-07	43.677000	-2.228000	marine	MAT on planktonic foraminifera	1/1/1 (2)	98 % (1)	59 yrs (1)	2	(Mary et al., 2017)
Monte Areo[b]	43.528889	-5.768889	terrestrial	pollen PCA	1/1/2 (2)	96 % (1)	480 yrs (3)	3	(López-Merino et al., 2010)
Kaite Cave	43.033333	-3.650000	speleothem	stalagmite $\delta^{13}C$	6/3/0 (1)	30 % (3)	10 yrs (1)	3	(Martín-Chivelet et al., 2011)
KGSC-31	43.006389	3.298889	marine	alkenones	1/4/2 (1)	99 % (1)	16 yrs (1)	1	(Jalali et al., 2016)
Cova da Arcoia	42.610000	-7.090000	speleothem	stalagmite $\delta^{18}O$	1/7/1 (1)	89 % (1)	67 yrs (1)	1	(Railsback et al., 2011)
Molinos Cave	40.792500	-4.492000	speleothem	Stalagmite $\delta^{18}O$	1/3/1 (1)	90 % (1)	31 yrs (1)	1	(Muñoz et al., 2015)
MD03-2699	39.036700	-10.660500	marine	alkenones	0/2/0 (2)	92 % (1)	154 yrs (2)	2	(Rodrigues et al., 2010)
D13882	38.634500	-9.454200	marine	alkenones	1/1/1 (2)	97 % (1)	112 yrs (2)	2	(Rodrigues et al., 2009)
D13902	38.554000	-9.335500	marine	alkenones	0/0/1 (3)	36 % (3)	271 yrs (3)	3	(Rodrigues et al., 2009)
MD01-2444	37.561333	-10.142167	marine	alkenones	0/0/0 (3)	96 % (1)	169 yrs (2)	3	(Martrat et al., 2007)
GeoB5901-2[a]	36.380000	-7.071333	marine	alkenones	3/12/1 (1)	79 % (2)	68 yrs (1)	2	(Schirrmacher et al., 2019)
M39008-3	36.380000	-7.071667	marine	alkenones	1/2/1 (2)	76 % (2)	456 yrs (3)	3	(Cacho et al., 2001)
HER_GC_T1	36.370146	-4.299015	marine	alkenones	0/1/1 (2)	95 % (1)	135 yrs (2)	2	(Ausín et al., 2015)
ODP-161-976A[a]	36.205333	-4.312667	marine	alkenones	0/11/0 (1)	91 % (1)	29 yrs (1)	1	(Schirrmacher et al., 2019)
ODP-161-976A[a,b]	36.205333	-4.312667	marine	pollen MAT	0/11/0 (1)	86 % (1)	259 yrs (3)	3	(Combourieu Nebout et al., 2009)
TTR-17_434G	36.205220	-4.312250	marine	alkenones	0/2/0 (2)	92 % (1)	129 yrs (2)	2	(Rodrigo-Gámiz et al., 2014)
TTR-12_293G	36.173567	-2.754667	marine	alkenones	0/1/0 (3)	83 % (1)	312 yrs (3)	3	(Rodrigo-Gámiz et al., 2014)
TTR-12_293G	36.173567	-2.754667	marine	TEX86	0/1/0 (3)	83 % (1)	312 yrs (3)	3	(Kim et al., 2015)
MD95-2043	36.143333	-2.621167	marine	alkenones	0/2/1 (2)	98 % (1)	117 yrs (2)	2	(Cacho et al., 1999)
ODP-161-977	36.031700	-1.955283	marine	alkenones	0/1/0 (3)	74 % (2)	553 yrs (3)	3	(Martrat et al., 2007)
summer									
PP10-07	43.677000	-2.228000	marine	MAT on planktonic foraminifera	1/1/1 (2)	98 % (1)	59 yrs (1)	2	(Mary et al., 2017)
SU92-03	43.195800	-10.113000	marine	MAT on planktonic foraminifera	1/0/0 (3)	83 % (1)	827 yrs (3)	3	(Salgueiro et al., 2014)
Basa de la Mora[b]	42.533333	0.316667	lake	chironomid assemblage	2/3/1 (1)	90 % (1)	300 yrs (3)	3	(Tarrats et al., 2018)
OMEXII-9K	42.343000	-10.051000	marine	MAT on planktonic foraminifera	0/1/0 (3)	83 % (1)	415 yrs (3)	3	(Salgueiro et al., 2014)
MD03-2697	42.150000	-9.700000	marine	MAT on planktonic foraminifera	1/1/0 (2)	71 % (2)	713 yrs (3)	3	(Salgueiro et al., 2014)
PO200-10-28-1	41.488000	-9.721000	marine	MAT on planktonic foraminifera	1/0/0 (3)	80 % (2)	803 yrs (3)	3	(Salgueiro et al., 2014)
MD95-2040	40.581833	-9.861167	marine	MAT on planktonic foraminifera	0/0/0 (3)	97 % (1)	242 yrs (3)	3	(Salgueiro et al., 2014)
MD95-2041	37.833333	-9.510833	marine	MAT on planktonic foraminifera	0/0/0 (3)	77 % (2)	463 yrs (3)	3	(Salgueiro et al., 2014)
MD95-2042	37.799833	-10.166500	marine	MAT on planktonic foraminifera	1/2/1 (2)	89 % (1)	332 yrs (3)	3	(Salgueiro et al., 2014)
GeoB5901-2[a]	36.380000	-7.071333	marine	MAT on planktonic foraminifera	3/12/1 (1)	100 % (1)	64 yrs (1)	1	(Schirrmacher et al., 2019)
ODP-161-976A[a]	36.205333	-4.312667	marine	MAT on planktonic foraminifera	0/11/0 (1)	84 % (1)	76 yrs (1)	1	(Schirrmacher et al., 2019)
ODP-161-976A[a,b]	36.205333	-4.312667	marine	pollen MAT	0/11/0 (1)	86 % (1)	259 yrs (3)	3	(Combourieu Nebout et al., 2009)
TTR-17_434G	36.205220	-4.312250	marine	LDI	0/2/0 (2)	95 % (1)	129 yrs (2)	2	(Rodrigo-Gámiz et al., 2014)

Name	Latitude	Longitude	Archive	Proxy	No. of datings preWin/Win/postWin (parameter-based QF)	Temporal coverage in Win (parameter-based QF)	Temporal resolution (parameter-based QF)	Final QF	References
TTR-12_293G	36.173567	-2.754667	marine	LDI	0/1/0 (3)	83 % (1)	312 yrs (3)	3	(Rodrigo-Gámiz et al., 2014)
MD99-2339	35.885500	-7.527833	marine	MAT on planktonic foraminifera	0/1/0 (3)	94 % (1)	401 yrs (3)	3	(Salgueiro et al., 2014)
Lake Sidi Ali[b]	33.050000	-5.000000	lake	*Cedrus*	2/5/1 (1)	94 % (1)	63 yrs (1)	1	(Campbell et al., 2017)
Tigalmamine	32.900000	-5.350000	lake	*Cedrus*	1/1/0 (2)	96 % (1)	107 yrs (2)	2	(Lamb and van der Kaars, 1995)
winter									
PP10-07	43.677000	-2.228000	marine	MAT on planktonic foraminifera	1/1/1 (2)	98 % (1)	59 yrs (1)	2	(Mary et al., 2017)
Lago de Ajo[a,b]	43.050000	-6.150000	lake	pollen MAT	0/1/0 (3)	94 % (1)	201 yrs (3)	3	(Allen et al., 1996)
Laguna de la Roya[a,b]	42.216667	-6.766667	lake	pollen MAT	0/1/1 (2)	90 % (1)	209 yrs (3)	3	(Allen et al., 1996)
Sanabria[a,b]	42.100000	-6.733333	lake	pollen MAT	0/0/0 (3)	94 % (1)	177 yrs (2)	3	(Allen et al., 1996)
MD95-2042[b]	37.799833	-10.166500	marine	MAT on planktonic foraminifera	1/2/1 (2)	90 % (1)	180 yrs (2)	2	(Chabaud et al., 2014)
GeoB5901-2[a]	36.380000	-7.071333	marine	MAT on planktonic foraminifera	3/12/1 (1)	100 % (1)	64 yrs (1)	1	(Schirrmacher et al., 2019)
ODP-161-976A[a]	36.205333	-4.312667	marine	MAT on planktonic foraminifera	0/11/0 (1)	84 % (1)	76 yrs (1)	1	(Schirrmacher et al., 2019)
ODP-161-976A[a,b]	36.205333	-4.312667	marine	pollen MAT	0/11/0 (1)	86 % (1)	259 yrs (3)	3	(Combourieu Nebout et al., 2009)

Artemisia are adapted to seasonal dry conditions and, thus, are indicative of prolonged annual dry periods (Cariñanos et al., 2004). Accordingly, an increase in xerophytic pollen percentage – either within a single of the above mentioned species or the sum of all three – was considered as reflecting annual dry conditions. Concerning the data of all non-pollen proxies, we follow the original interpretation of the authors. This also includes the interpretation of *Cedrus* pollen percentages in northern Africa, where an increase indicates decreasing summer temperatures (Lamb and van der Kaars, 1995; Campbell et al., 2017).

Age models for the new marine records of cores OD-161-976A and GeoB5901-2 (Fig. S3; Schirrmacher et al., 2019) were updated with 5 and 6 new AMS ^{14}C dates, respectively, and have been calculated using the Bacon package (Blaauw and Christen, 2011) in the R programming language (R Core Team, 2019). The new AMS ^{14}C dates were measured at the Leibniz Laboratory at Kiel University (Table S1).

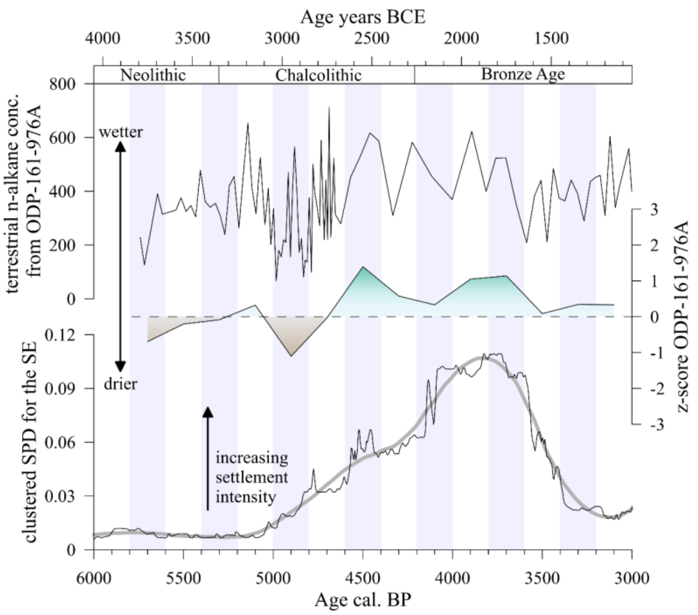

Fig. 2. Illustration of the methodological approach. At the top the concentration of terrestrial n-alkanes (n-C_{27-33}) of marine sediment core ODP-161-976A from the Alboran Sea (Schirrmacher et al., 2019) with the updated age model (see Fig. S3) is shown. In the centre the according medians of the z-transformed data are shown for the 200-year time slices (blue vertical bars). The green and brown shadings indicate the intensity of wetter or drier conditions, respectively. At the bottom raw data of clustered summed probability densities (SPDs) for the southeast (SE) of the Iberian Peninsula are displayed in black together with a LOESS smooth in grey (see Fig. 1 for location).

For the analysis only palaeoclimatic data between 6000 and 3000 cal. BP (4050 – 1050 BCE) have been compiled. For each dataset the z-score (Clark-Carter, 2014) has been calculated to achieve comparability among all proxies. Depending on the variable, a positive (negative) score indicates relatively humid (dry) or warm (cool) conditions, respectively, in relation to the average conditions of each record between 6000 and 3000 cal. BP (4050 – 1050 BCE). The higher (positive or negative) the score, the more pronounced the respective climatic conditions. Afterwards, medians of 200-year time slices within the interval have been calculated for each proxy. For an illustration of the methodological approach please see Figure 2.

Considering the wide range of important parameters within the compiled palaeoclimatic data, such as temporal resolution, coverage of the studied time period, and number of datings, we assigned a quality flag (QF) to each record based on the above mentioned parameters. The QF ranges from 1 to 3 and was calculated separately for every parameter (number of datings, temporal resolution, and temporal coverage). The thresholds for every parameter are shown in Table 2. The final QF is then based on the lowest QF of all parameters. For example, a well-dated record with decadal resolution (QFs of 1 for number of datings and temporal resolution), which covers less than half of the studied period (QF of 3 for temporal coverage), received a final QF of 3. Given the relatively high spatial coverage of annual and winter precipitation data, we interpolated the data in order to highlight areas of coherent regional developments. This was done by inverse distance weighting interpolation of the individual z-scores using packages gstat (Pebesma, 2004) and raster (Hijmans, 2019) within R software (R Core Team, 2019). Thereby, we weighted the data according to its final QF to account for the different quality of each record during interpolation. Records with a QF of 1 were taken into account with a factor of 3, while records with a QF of 2 received a factor of 2. During interpolation we used a power value of 1.5 while the search radius was not limited. Unfortunately, the spatial coverage of all other variables was insufficient for reasonable interpolations. Animations showing the development of all six palaeoclimatic reconstructions for the whole time period can be found in the supplement of this article (Videos S1 – S6).

Table 2
Quality flag parameters. The assignment of the final quality flag (QF) is described in the text. preWin = 2000 – 3000 cal. BP (50 – 1050 BCE); Win = 3000 – 6000 cal. BP (1050 – 4050 BCE); postWin = 6000 – 7000 cal. BP (4050 – 5050 BCE)

QF	Average temporal resolution	Number of datings in 2000 – 7000 cal. BP (50 – 5050 BCE)	Temporal coverage (3000 – 6000 cal. BP/ 1050 – 4050 BCE)
1	> 100 years	≥ 5 with at least 3 in Win	> 80 %
2	≥ 200 years	≥ 2 with either at least 1 in Win or 1/1 in preWin and postWin	≥ 50 %
3	< 200 years	< 2	< 50 %

2.2 Archaeological approach

In this paper, we use summed probability densities (SPDs) of AMS ^{14}C dates from archaeological contexts to infer past human activity on the Iberian Peninsula (Fig. 1). SPDs are used as a preferred proxy for the past human activity as it provides a high temporal and spatial resolution, and allows for supra-regional comparison. Due to potential (and inevitable) biases related to the shape of the ^{14}C calibration curve and the focus of archaeological research, the use of this proxy is critically debated (Williams, 2012; Contreras and Meadows, 2014; Weninger et al., 2015). Nonetheless, its successful and intensive use, which is paralleled by a rapidly growing AMS ^{14}C database, is well documented in recent literature and enables increasingly robust reconstructions and safer interpretations (Hinz et al., 2012a; Lillios et al., 2016; Drake et al., 2017; Warden et al., 2017; Blanco-González et al., 2018). In order to avoid biases from changes in the cultural behaviour of the societies samples from funeral and ritual contexts were left out, and only samples from settlement context were retained in the database (Hinz et al., 2012a). Iberian AMS ^{14}C data have been compiled from existing datasets (IDEArq (n.d.); Hinz et al., 2012b; Kneisel et al., 2013) and complemented with other published data (Lillios et al., 2016). The data have been carefully checked for duplicate dates before analysis to avoid over-representation of well-researched sites. For further analysis, AMS ^{14}C dates between 7000 and 2000 uncalibrated (uncal.) BP (5050 – 50 uncal. BCE) have been taken into account in order to ensure that the calibrated dates fall within the analysed period between 6000 and 3000 cal. BP (4050 – 1050 BCE). In this (uncalibrated) timeframe, our database contains 4710 dates from 880 settlements covering the entire Iberian Peninsula. Calibration of AMS ^{14}C data and SPD computation was done using INTCAL13 calibration curve (Reimer et al., 2013) and the rcarbon package (Crema et al., 2017; Bevan and Crema, 2018), and using the R programming language (R Core Team, 2019). Prior to sum-calibration the calibrated data were binned by site and the resulting site-SPDs have then been normalized to unity, in order to achieve comparability between all sites, and to minimize bias potentially resulting from different research intensity (Hinz et al., 2012a). Nonetheless, biases introduced into the reconstructed spatial patterns by different archaeological research intensities cannot be fully eliminated and, thus, unavoidably affect the outcome.

After computing the site-SPDs, medians of each site were calculated for 200-year time slices between 6000 and 3000 cal. BP (4050 – 1050 BCE) to match the resolution of the climate compilations (Fig. 2). The advantage of medians is that their calculation is not as dependent on outlier (or minima and maxima) as the calculation of mean values. Hence, this also minimizes an effect pointed out by Weninger et al. (2015) where the normalization of sum-calibrated dates may produce false peaks related to the calibration curve and, thus, increases the reliability of our results. For each time slice a heat map based on the distances between settlements and the respective SPD of each site was calculated. An animation showing the development of the settlement density within the whole time period can be found in the supplement of this article (Video S7).

3. Results and Discussion

3.1 Settlement intensity variability during the Chalcolithic and Bronze Age on the Iberian Peninsula

The settlement pattern during the Chalcolithic and the Bronze Age as reconstructed from spatial SPD analyses reveal new insights into the spatio-temporal developments of specific regions of the Iberian Peninsula. Overall, our results imply high human activities in the southern part of the peninsula during the analysed period, which agree well with the development of major archaeological cultures of the time. Thus, this further enables the use of SPDs as indicator for demographic and settlement developments on the southern Iberian Peninsula at that time.

A high settlement density developed after 5600 cal. BP (3650 BCE) in the Alentejo and Algarve near the Atlantic coast (Fig. 3) and lasted until 4200 cal. BP (2250 BCE) (Fig. 4; Video S7). Nucleation of settlements during this phase is well supported by aoristic analysis of settlement patterns in the Alentejo and Algarve regions (Hinz et al., 2019). In this late Chalcolithic phase, the walled site of Zambujal has been constructed in the area (Kunst and Lutz, 2008) contemporaneous with the overall increasing settlement density in the SW. After 4800 cal. BP (2850 BCE) settlement intensity gradually shifted towards the SE, where the Los Millares culture had already emerge since 5150 cal. BP (3200 BCE) (Fig. 3; Molina González et al., 2004). According to our SPD data, both societies in the SW and the SE were co-existing until ca. 4200 cal. BP (2250 BCE), when SPDs sharply dropped in the SW and settlements in the Alentejo and Algarve virtually disappeared (Fig. 4). Yet, this final "collapse" was preceded by a gradual decline in SPD values starting from 4400 cal. BP (2450 BCE) onwards (Video S7) in line with archaeological studies from Zambujal and Perdigões (Kunst and Lutz, 2008; Valera, 2015). Based on regional-clustered SPDs from settlement and burial contexts, Lillios et al. (2016) have argued previously that the decrease in demographic signals in the SW started around 4500 cal. BP (2550 BCE) and considered the possibility of demic migration towards the east. But, also in the SE various settlement sites have been abandoned, among them well investigated mega-sites like Los Millares, Valencina de la Concepción, or Marroquíes Bajos coinciding with the disappearance of the Los Millares culture (Lull et al., 2015; García Sanjuán et al., 2018). Jointly, the large-scale abandonment of settlement sites and the vanishing of traditions in material culture and burial rites implies that the southern part of the Iberian Peninsula featured a regional-wide social collapse around 4200 cal. BP (2250 BCE).

Nonetheless, the settlement intensity in the SE intensified and spread northward along the Mediterranean coast and into the southern Meseta area after 4200 cal. BP (2250 BCE) (Fig. 4). This development is associated with the boom of the El Argar culture (Lull et al., 2011). Human activity in the southern Meseta area is, further, associated with the construction of the *motillas* in the floodplains of the Guadiana and Guadalquivir river basins (Aranda et al., 2008; Benítez de Lugo Enrich and Mejías, 2017). In line with Lull et al. (2011), our data suggest that the Argaric territory reached its maximum between 3800 and 3600 cal. BP (1850 – 1650 BCE) and its bust started after ca. 3600 cal. BP (1650 BCE) with the majority of settlement sites in the area being abandoned by 3400 cal. BP (1450 BCE) (Fig. 4 and Video S7).

According to our SPD analyses two periods of interesting settlement patterns stand out and are discussed in the following chapters. The first period ranges from 5200 to 4600 cal. BP (3250 – 2650 BCE) and comprised the development of the co-existing societies in the SW and the SE. The second period from 4400 to 3400 cal. BP (2450 – 1450 BCE) featured the collapse in the SW and the boom and bust of the El Argar culture in the SE. Comparing these settlement patterns with the compiled palaeoclimatic data, we explore whether the subsequent development of the societies in the SW and the SE during the Chalcolithic, which potentially featured a population migration (Lillios et al., 2016), was favoured by more pleasant climatic conditions in the SE. Also, after resolving the spatio-temporal manifestation of the 4.2 ka BP climate event across the Iberian Peninsula we explore its potential impact on the social collapse at that time in the SW and the following demographic boom associated with the El Argar culture in the SE.

3.2 Development of two settlement hotspots between 5200 – 4600 cal. BP (3250 – 2650 BCE)

The development of the society in the SW after 5600 cal. BP (3650 BCE) and the subsequent rise of the Los Millares culture after 4800 cal. BP (2850 BCE) were accompanied by profound climatic changes between 5000 and 4800 cal. BP (3050 – 2850 BCE) (Fig. 3). Although likely not dramatic, the majority of annual temperature records in this time slice suggests a peninsular-wide cooling. The few seasonal temperature records available suggest that people had to deal rather with a winter cooling (Videos S2 and S3). Regarding the hydro-climatic conditions, it has been relatively moist in the annual mean between 5200 and 4600 cal. BP (3250 – 2650 BCE) with the exception of a regional drying across the northern Iberian Peninsula at the end of this phase (Fig. 3). The overall relatively moist annual and winter conditions during that period reflect the long-term Holocene drying trend towards the present, rather than a particular wet event (Videos S4 and S5). Nonetheless, while annual conditions were relatively moist from 5000 to 4800 cal. BP (3050 – 2850 BCE), winter precipitation likely decreased during this phase as for example indicated by marine core GeoB5901-2 from the Gulf of Cadiz (Schirrmacher et al., 2019). This decrease in winter precipitation was more pronounced along the Atlantic coast including the SW area (Fig. 3).

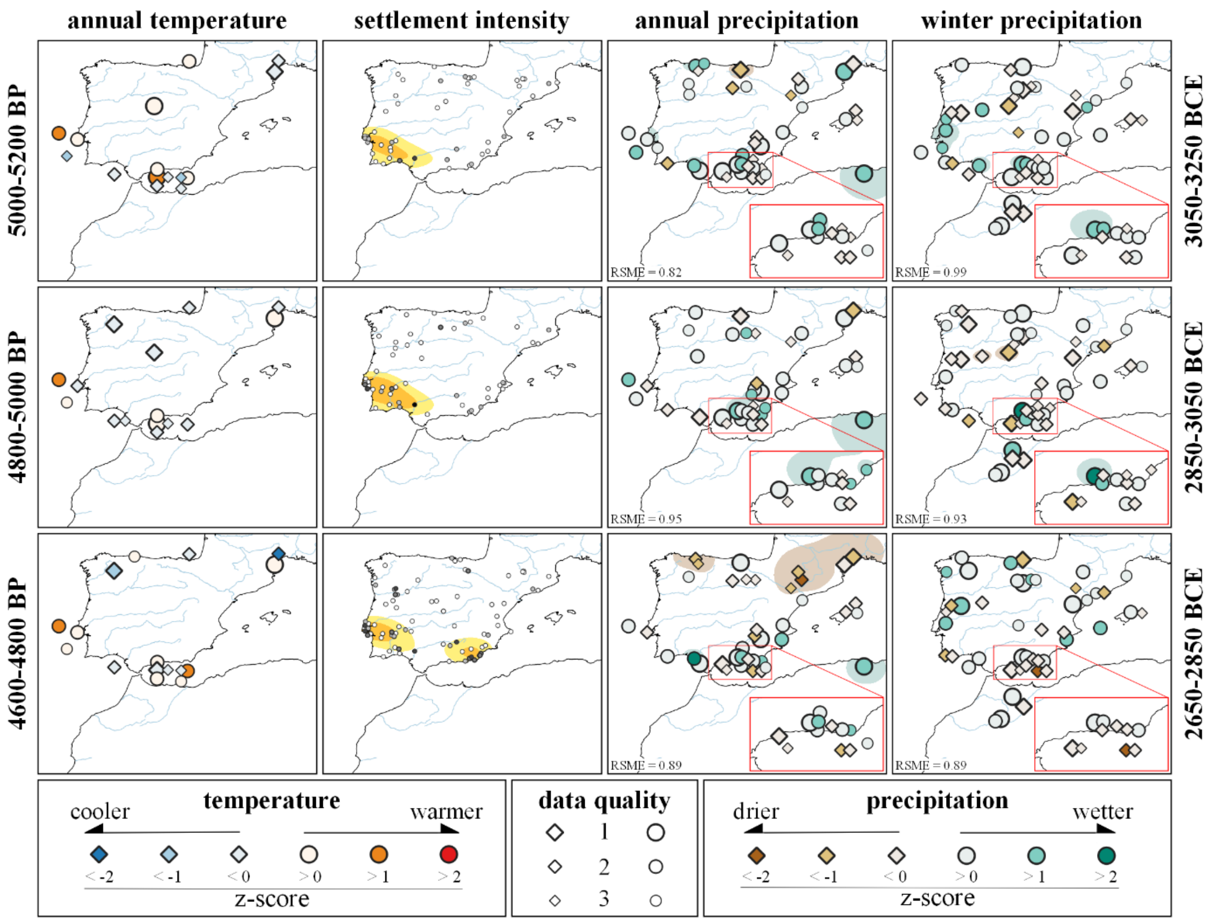

Fig. 3. Climatic and archaeological proxy data for the time slices between 5200 to 4600 cal. BP (3250 – 2650 BCE). From left to right: annual temperatures, settlement intensities, annual precipitation and winter precipitation reconstructions. The heatmap in the settlement intensity column (from yellow to red colours) were calculated using the settlement density as well as the SPD data of each settlement. The brown and green shadings in the annual and winter precipitation data highlight areas of regional change towards drier or wetter conditions, respectively, based on inverse distance weighted interpolation of the z-score data.

Accordingly, it is interesting to note that the rise of the Los Millares culture in the SE was preceded by a cool and dry winter event, which was particularly manifested in the SW. At this time economies across the southern Iberian Peninsula were highly dependent on agriculture and, consequently, arable land (García Sanjuán et al., 2016; Schneider et al., 2016; López-Sáez et al., 2018). Moreover, irrigation was likely not practised before 4300 cal. BP (2350 BCE) in the area, highlighting the importance of natural water resources (Mora-González et al., 2016; Benítez de Lugo Enrich and Mejías, 2017; Mora-González et al., 2018).

Thus, following the idea that this cool and dry winter event between 5000 and 4800 cal. BP (3050 – 2850 BCE) hampered the agricultural production in the SW, it appears plausible that the rise of the Los Millares culture in the SE after 4800 cal. BP (2850 BCE) was favoured by climatic-induced migration from the SW. Lillios et al. (2016) already suggested a potential migration after ca. 4500 cal. BP (2550 BCE) from the SW towards the SE. Strontium isotopic analysis ($^{87/86}Sr$) of human teeth indeed suggest that a variable amount of non-local population at the Andalusian mega-sites Marroquíes Bajos and Valencina de la Concepción entered existing social networks (Díaz-Zorita Bonilla, 2013; Díaz-Zorita Bonilla et al., 2018). The provenance of such groups remain an open question, though. While it is unlikely that people moved eastwards for metals and related economic reasons (Bartelheim and Pearce, 2015), it might be possible that the establishment of trade networks as evidenced by the arrival of Asian ivory favoured migration towards the SE (Schuhmacher, 2017).

Following these lines of evidence, climatic-induced migration related to a cool and dry winter event, particularly evident in the SW, likely contributed to the observed gradual displacement of settlement intensities from the SW towards the SE after 4800 cal. BP (2850 BCE).

3.3 Boom and bust on the southern Iberian Peninsula between 4400 – 3400 cal. BP (2450 – 1450 BCE)

The period between 4400 and 3400 cal. BP (2450 – 1450 BCE) is characterized by two distinct climatic events, which superimpose the general drying and cooling trends. Particularly, we observe increasingly drier conditions across the southern Iberian Peninsula from 3800 to 3000 cal. BP (1850 – 1050 BCE). These are reflected in the annual reconstructions (Video S4), but clearly forced by decreasing winter precipitation (Video S5). This decrease in winter precipitation is likely related to the drying trend during the Holocene and, thus, is very different from the two earlier events.

During the first event, which occurred between 4400 and 4000 cal. BP (2450 – 2050 BCE), the whole Iberian Peninsula faced cooler annual conditions (Fig. 4). Contrastingly, the alkenone record of GeoB5901-2 from the Gulf of Cadiz suggests distinctly warmer annual sea surface temperatures by 2 °C. But, this may be rather a result of a shift in the growing season of the alkenone producers in response to altered seasonality and nutrient conditions (Schirrmacher et al., 2019). Seasonal temperature data based on pollen and planktonic foraminiferal assemblages implies that the annual cooling was likely a result of cooler winter conditions, while summer temperatures were relatively constant (Videos S2 and S3). Altogether, this suggests a decrease in seasonality during this event. Paralleling the winter cooling between 4400 and 4000 cal. BP (2450 – 2050 BCE), hydroclimatic conditions across the Iberian Peninsula were rather stable indicating no event-like features (Fig. 4). Decreasing annual or winter precipitation as suggested by two offshore marine records based on n-alkane concentrations or localized pollen data between 4200 and 4000 cal. BP (2250 – 2050 BCE) rather mirror altered sediment transport pathways into the marine realm or anthropogenic forest clearance, respectively.

Thus, the period from 4400 to 4000 cal. BP (2450 – 2050 BCE) is characterized by a winter cooling event, which is contemporaneous with a major ice-berg discharge in the North Atlantic – the so-called Bond Event 3 (Bond et al., 2001). This, further, corroborates the hypothesis by

Schirrmacher et al. (2019) that cooling during Bond Event 3 close to the Iberian Atlantic coast was a winter phenomenon. Our data also indicates that Bond Event 3 was not associated with a regional decrease in precipitation on the Iberian Peninsula.

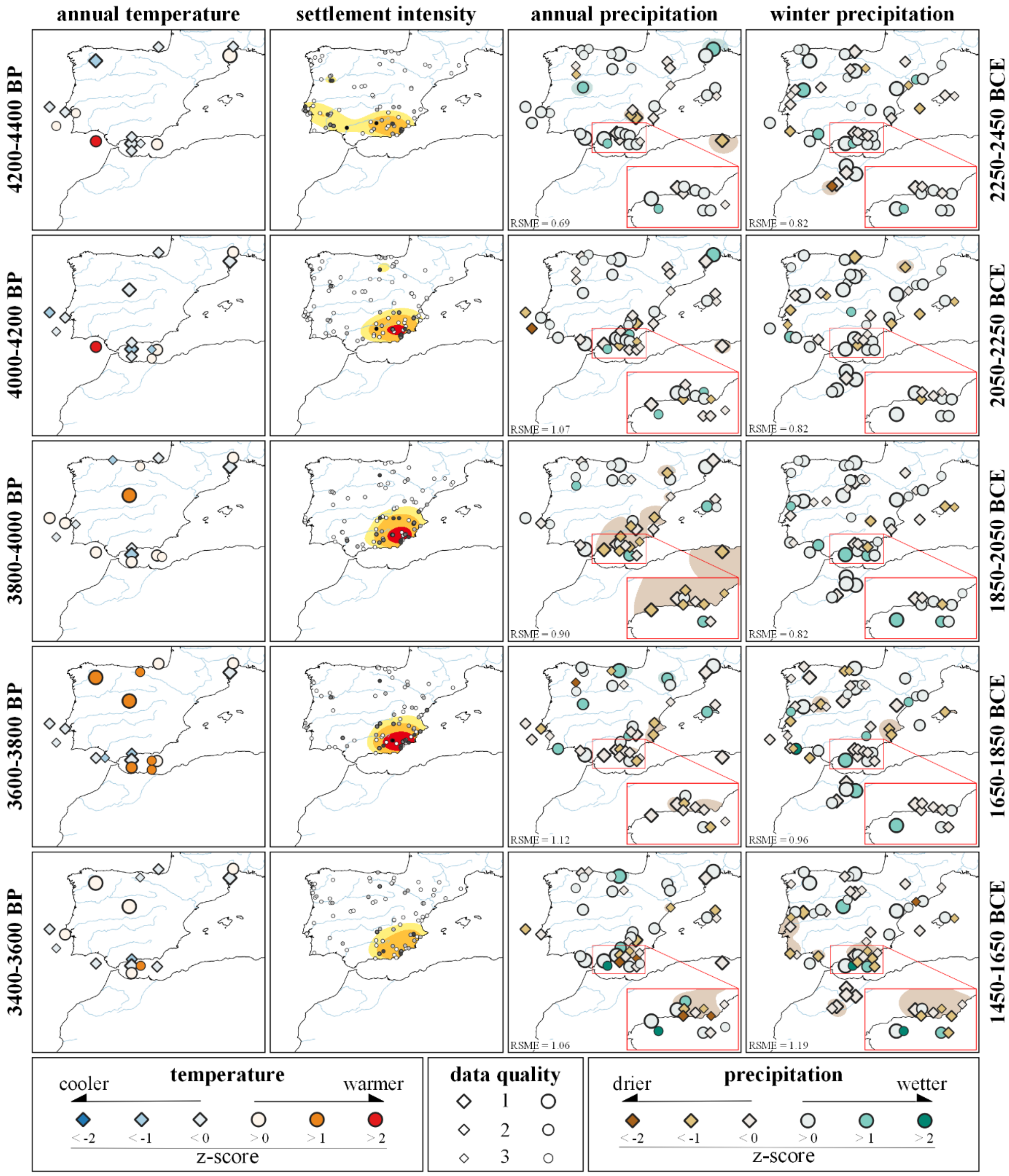

Fig. 4. Climatic and archaeological proxy data for the time slices between 4400 to 3400 cal. BP (2450 – 1450 BCE). From left to right: annual temperatures, settlement intensities, annual precipitation and winter precipitation reconstructions. The heatmap in the settlement intensity column (from yellow to red colours) were calculated using the settlement density as well as the SPD data of each settlement. The brown and green shadings in the annual and winter precipitation data highlight areas of profound regional change towards drier or wetter conditions, respectively, based in inverse distance weighted interpolation of the z-score data.

Having discussed the first climatic event of the period between 4400 and 3400 cal. BP (2450 – 1450 BCE), we can now turn to the second event, which abruptly occurred between 4000 and 3800 cal. BP (2050 – 1850 BCE). During this period, the hydroclimatic data points to a sharp decrease in annual precipitation in the SE, while winter precipitation in the area remains relatively constant or even increased (Fig. 4). This leads to the conclusion that this event was probably driven by a sharp decrease in summer precipitation or an elongation of the summer dry period. Despite just two compiled archives are indicative of summer precipitation variability, a regional decrease in summer precipitation in the SE is suggested by pollen-based MAT reconstruction in marine sediment core MD95-2043 from the Alboran Sea (Video S6) (Bini et al., 2019). Thus, this event noticeably differs from the drying trend, which is evident afterwards and characterized by a decrease in winter precipitation (Fig. 4; Video S5). At the same time, the western and northern Atlantic coasts faced stable annual precipitation levels, pointing to a strong Atlantic – Mediterranean gradient and a potential Mediterranean forcing of the summer dry event between 4000 and 3800 cal. BP (2050 – 1850 BCE).

In light of the 4.2 ka BP drought event, which is described for the period between 4300 to 3800 cal. BP (2350 – 1850 BCE) in the Central and Eastern Mediterranean (Kaniewski et al., 2018; Bini et al., 2019), we suggest that this event had a shorter duration (4000 – 3800 cal. BP; 2050 – 1850 BCE) and just affected the Mediterranean coast – the SE in particular – of Iberian Peninsula. Moreover, the 4.2 ka BP drought event in the area was likely restricted to the summer season.

The 4.2 ka BP drought event is known for contributing to social collapse and large-scale population displacements in the Near East (Welc and Marks, 2014; Weiss, 2017). Therefore, it is interesting to note that social developments, among them the large-scale abandonment of settlement sites on the southern Iberian Peninsula around 4200 cal. BP (2250 BCE), are indicative of a collapse as well (Lull et al., 2015; Valera, 2015). But, from our palaeoclimatic data it appears that the 4.2 ka BP event was not directly affecting societies in the SW and the

SE at that time. On the southern Iberian Peninsula, the 4.2 ka BP event occurred later (4000 – 3800 cal. BP; 2050 – 1850 BCE) and had likely not impacted the SW at all (Fig. 4). This is corroborated by Valera et al. (2015), who proposed that the abandonment of ditched enclosures in the SW was not driven by climatic factors. The SE, on the other hand, even featured the boom of the El Argar culture at that time (Lull et al., 2011) despite the dry summer conditions associated with the regional manifestation of the 4.2 ka BP event and the abandonment of Chalcolithic sites. Multiple lines of evidence suggest that the Argaric people were able to deal with dry summer conditions during the 4.2 ka BP event as indicated by agricultural practises, which are based on dry farming, monoculture (Castro et al., 1999; Delgado-Raack and Risch, 2015), and/or irrigation techniques (Mora-González et al., 2016; Benítez de Lugo Enrich and Mejías, 2017). In addition, our palaeoclimatic data suggests that the stable or increased winter precipitation during this phase supported people in maintaining the intensive agricultural production (Fig. 4).

Interestingly, during the collapse of the Argaric society between 3600 and 3500 cal. BP (1650 – 1550 BCE) (Lull et al., 2013b) an over-regional decrease in winter precipitation across the southern Iberian Peninsula becomes evident from various terrestrial and marine pollen records as well as speleothem data (Fig. 4). So far, it has been suggested that the collapse of the Argaric society was caused by the extensive over-exploitation of the environment including intense woodland clearance (Castro et al., 1999; Lull et al., 2013a, 2013b). This may account for the decrease in winter precipitations mirrored by some localized pollen data from the SE between 3600 and 3400 cal. BP (1650 – 1450 BCE). But, a decrease in winter precipitation is also suggested from speleothem data and marine pollen records. Furthermore, pollen data from the SW, where human activity was limited according to our SPD analysis, also imply dry winter conditions. Altogether, a regional-wide decrease in winter precipitation across the southern Iberian Peninsula is suggested already after 3800 cal. BP (1850 BCE). Accordingly, we conclude that during the boom of the Argaric culture its society was increasingly dependent on winter precipitation in order to maintain the intense agriculture. Thus, a significant decrease in winter precipitation after 3800 cal. BP (1850 BCE) likely contributed to the collapse of the El Argar culture by hampering the intense agricultural practises.

4. Conclusion

In order to fill important knowledge gaps concerning a potential link between climate change and social developments during the Chalcolithic and the Bronze Age on the Iberian Peninsula, we compiled palaeoclimatic and archaeological data from the time period between 6000 to 3000 cal. BP (4050 – 1050 BCE) from the Iberian Peninsula. The palaeoclimate was analysed for seasonal (summer and winter) and annual variability in precipitation as well as temperature. Sum-calibrated probability densities (SPDs) of AMS ^{14}C data served as proxy for settlement intensity.

The results of the SPD analysis indicate an increase in settlement intensity in the southwest (SW) of the Iberian Peninsula after 5600 cal. BP (3650 BCE) and a subsequent rise in settlement density in the adjacent southeast (SE) after 4800 cal. BP (2850 BCE), which is associated with the Los Millares culture. While settlement intensity in the SW sharply declined around 4200 cal. BP (2250 BCE), increasing settlement activity related to the emerging El Argar culture is indicated for the SE until ca. 3600 cal. BP (1650 BCE).

The palaeoclimatic analysis resolved the long-term Holocene aridification trend on the Iberian Peninsula. This trend is primarily associated with a gradual decrease in winter precipitation and culminates after ca. 3800 cal. BP (1850 BCE), when particularly the southern Iberian Peninsula faced dry winter conditions. The aridification trend is superimposed by the 4.2 ka BP climate event from 4000 to 3800 cal. BP (2050 – 1850 BCE). During the event the SE was affected by an abrupt decrease in summer precipitation or an elongation of the summer dry period, while winter precipitation remained rather constant. With respect to temperature, the Iberian

Peninsula experienced winter cooling between 4400 and 4000 cal. BP (2450 – 2050 BCE) in phase with Bond Event 3.

Comparing settlement patterns and the distribution of precipitation, we found no direct link between the large-scale abandonment of settlement sites in the SW around 4200 cal. BP (2250 BCE) and the 4.2 ka BP climate event. But, we noticed that the Chalcolithic and Bronze Age societies of the southern Iberian Peninsula were highly dependent on winter precipitation to maintain their agricultural practises. For instance, the decline in settlement intensity in the SW around 4800 cal. BP (2850 BCE) was preceded by a reduce in winter precipitation in the area. Furthermore, a sharp decrease in winter precipitation also coincides with the bust of the El Argar culture in the SE after 3600 cal. BP (1650 BCE). Before, between 4000 and 3800 cal. BP (2050 – 1850 BCE), the Argaric society boomed during the enhanced summer drought associated with the regional manifestation of the 4.2 ka BP event. This further highlights the dependence on winter precipitation of the southern Iberian societies during the Chalcolithic and Bronze Age.

5. Outlook

Apart from the results and conclusions, this study has also highlighted the need of much more well-dated, high-resolution palaeoclimate data. Especially, seasonal data have an insufficient spatial resolution, but also in the annual data some regions, for example the Alentejo, Extremadura, and Algarve are not well researched. In the marine realm, the northern Atlantic and western Mediterranean coasts are clearly underrepresented. From the archaeological perspective surely more fieldwork should be carried out in the northern part of the Iberian Peninsula, in order to better understand why these regions are characterized by relative stability during the Chalcolithic and the Bronze Age. Also, there is a need for detailed archaeo-botanical and dietary studies to significantly improve the knowledge of agricultural practises in the past.

This knowledge will be needed for better comparability of social and palaeoclimatological variability on the Iberian Peninsula.

Acknowledgements

This research was performed in the framework of the CRC 1266 “Scales of transformation” (project number: 2901391021) funded by the DFG (German Research Foundation). The authors acknowledge the tremendous work of the databases (European Pollen Database, Pangaea, NOAA Paleo Data Search, SISAL, and IDEArq) from which the data for this study have been compiled. In this respect, we also want to thank Gianni Zanchetta and Monica Bini for providing data. We are also grateful for help with the archaeological analysis by Jan-Eric Schlicht and Ingo Feeser. Additionally, we thank Eileen Kücükkaraca for editing and improving the English language.

Appendix A. Supplementary data.

Appendix B. Supplementary videos.

The authors declare that they have no conflict of interest.

References

Abel Schaad, D., Hernández Carretero, A.M., López Sáez, J.A., Pulido Díaz, F.J., López Merino, L., Martínez Cortizas, A., 2009. Evolución de la vegetación en la Sierra de Gata (Cáceres-Salamanca, España) durante el Holoceno reciente.: Implicaciones biogeográficas. Revista Española de Micropaleontología 41(1-2), 91–105.

Abel-Schaad, D., López-Sáez, J.A., 2013. Vegetation changes in relation to fire history and human activities at the Peña Negra mire (Bejar Range, Iberian Central Mountain System, Spain) during the past 4,000 years. Veget Hist Archaeobot 22(3), 199–214. doi:10.1007/s00334-012-0368-9.

Ait Brahim, Y., Wassenburg, J.A., Sha, L., Cruz, F.W., Deininger, M., Sifeddine, A., Bouchaou, L., Spötl, C., Edwards, R.L., Cheng, H., 2019. North Atlantic Ice-Rafting, Ocean and Atmospheric Circulation During the Holocene: Insights From Western Mediterranean Speleothems. Geophys. Res. Lett. 4, 150. doi:10.1029/2019GL082405.

Allen, J.R.M., Huntley, B., Watts, W.A., 1996. The vegetation and climate of northwest Iberia over the last 14,000 years. J. Quaternary Sci. 11(2), 125–147.

Anderson, R.S., Jiménez-Moreno, G., Carrión, J.S., Pérez-Martínez, C., 2011. Postglacial history of alpine vegetation, fire, and climate from Laguna de Río Seco, Sierra Nevada, southern Spain. Quaternary Science Reviews 30(13-14), 1615–1629. doi:10.1016/j.quascirev.2011.03.005.

Aranda, G., Fernández, S., Haro, M., Molina, F., Nájera, T., Sánchez, M., 2008. Water control and cereal management on the Bronze Age Iberian Peninsula: La motilla del Azuer. Oxford Journal of Archaeology 27(3), 241–259. doi:10.1111/j.1468-0092.2008.00306.x.

Atsawawaranunt, K., Harrison, S., Comas-Bru, L., 2019. SISAL (Speleothem Isotopes Synthesis and AnaLysis Working Group) database version 1b. University of Reading.
Ausín, B., Flores, J.A., Sierro, F.J., Cacho, I., Hernández-Almeida, I., Martrat, B., Grimalt, J.O., 2015. Atmospheric patterns driving Holocene productivity in the Alboran Sea (Western Mediterranean): A multiproxy approach. The Holocene 25(4), 583–595. doi:10.1177/0959683614565952.
Bartelheim, M., Pearce, M., 2015. Early Metallurgy in Iberia and the Western Mediterranean. In: Fowler, C., Harding, J., Hofmann, D. (Eds.), The Oxford Handbook of Neolithic Europe. Oxford University Press, Oxford.
Benítez de Lugo Enrich, L., Mejías, M., 2017. The hydrogeological and paleoclimatic factors in the Bronze Age Motillas Culture of La Mancha (Spain): The first hydraulic culture in Europe. Hydrogeol J 25(7), 1931–1950. doi:10.1007/s10040-017-1607-z.
Bevan, A., Crema, E.R., 2018. rcarbon: Methods for calibrating and analysing radiocarbon dates.
Bini, M., Zanchetta, G., Perşoiu, A., Cartier, R., Català, A., Cacho, I., Dean, J.R., Di Rita, F., Drysdale, R.N., Finnè, M., Isola, I., Jalali, B., Lirer, F., Magri, D., Masi, A., Marks, L., Mercuri, A.M., Peyron, O., Sadori, L., Sicre, M.-A., Welc, F., Zielhofer, C., Brisset, E., 2019. The 4.2 ka BP Event in the Mediterranean region: An overview. Clim. Past 15(2), 555–577. doi:10.5194/cp-15-555-2019.
Blaauw, M., Christen, J.A., 2011. Flexible paleoclimate age-depth models using an autoregressive gamma process. Bayesian Anal. 6(3), 457–474. doi:10.1214/11-BA618.
Blanco-González, A., Lillios, K.T., López-Sáez, J.A., Drake, B.L., 2018. Cultural, Demographic and Environmental Dynamics of the Copper and Early Bronze Age in Iberia (3300–1500 BC): Towards an Interregional Multiproxy Comparison at the Time of the 4.2 ky BP Event. J World Prehist 31(1), 1–79. doi:10.1007/s10963-018-9113-3.
Bond, G., Kromer, B., Beer, J., Muscheler, R., Evans, M.N., Showers, W., Hoffmann, S., Lotti-Bond, R., Hajdas, I., Bonani, G., 2001. Persistent solar influence on North Atlantic climate during the Holocene. Science (New York, N.Y.) 294(5549), 2130–2136. doi:10.1126/science.1065680.
Burjachs, F., Expósito, I., 2015. Charcoal and pollen analysis: Examples of Holocene fire dynamics in Mediterranean Iberian Peninsula. CATENA 135, 340–349. doi:10.1016/j.catena.2014.10.006.
Burjachs, F., Giralt, S., Roca, J.R., Seret, G., Julià, R., 1997. Palinología holocénica y desertización en el Mediterráneo occidental. In: Ibañez, J.J., Valero, B.L., Machado, C. (Eds.), El paisaje mediterráneo a través del espacio y del tiempo.: Implicaiones en la desertificación. Geoforma Editores, Logroño, pp. 379–394.
Cacho, I., Grimalt, J.O., Canals, M., Sbaffi, L., Shackleton, N.J., Schönfeld, J., Zahn, R., 2001. Variability of the western Mediterranean Sea surface temperature during the last 25,000 years and its connection with the Northern Hemisphere climatic changes. Paleoceanography 16(1), 40–52. doi:10.1029/2000PA000502.
Cacho, I., Grimalt, J.O., Pelejero, C., Canals, M., Sierro, F.J., Flores, J.A., Shackleton, N., 1999. Dansgaard-Oeschger and Heinrich event imprints in Alboran Sea paleotemperatures. Paleoceanography 14(6), 698–705. doi:10.1029/1999PA900044.
Campbell, J.F.E., Fletcher, W.J., Joannin, S., Hughes, P.D., Rhanem, M., Zielhofer, C., 2017. Environmental Drivers of Holocene Forest Development in the Middle Atlas, Morocco. Front. Ecol. Evol. 5, 201. doi:10.3389/fevo.2017.00113.
Cariñanos, P., Galan, C., Alcázar, P., Domínguez, E., 2004. Airborne pollen records response to climatic conditions in arid areas of the Iberian Peninsula. Environmental and Experimental Botany 52(1), 11–22. doi:10.1016/j.envexpbot.2003.11.008.
Carrión, J.S., 2002. Patterns and processes of Late Quaternary environmental change in a montane region of southwestern Europe. Quaternary Science Reviews 21(18-19), 2047–2066. doi:10.1016/S0277-3791(02)00010-0.
Carrión, J.S., Andrade, A., Bennett, K.D., Navarro, C., Munuera, M., 2001a. Crossing forest thresholds: inertia and collapse in a Holocene sequence from south-central Spain. The Holocene 11(6), 635–653.

Carrión, J.S., Munuera, M., Dupré, M., Andrade, A., 2001b. Abrupt vegetation changes in the Segura Mountains of southern Spain throughout the Holocene. J Ecol 89(5), 783–797. doi:10.1046/j.0022-0477.2001.00601.x.

Carrión, J.S., Sánchez-Gómez, P., Mota, J.F., Yll, R., Chaín, C., 2003. Holocene vegetation dynamics, fire and grazing in the Sierra de Gádor, southern Spain. The Holocene 13(6), 839–849. doi:10.1191/0959683603hl662rp.

Carrión, J.S., Yll, E.I., Willis, K.J., Sánchez, P., 2004. Holocene forest history of the eastern plateaux in the Segura Mountains (Murcia, southeastern Spain). Review of Palaeobotany and Palynology 132(3-4), 219–236. doi:10.1016/j.revpalbo.2004.07.002.

Castro, P.V., Chapman, R.W., Gili, S., Lull, V., Micó, R., Rihuete, C., Risch, R., Sanahuja, M.E., 1999. Agricultural production and social change in the Bronze Age of southeast Spain: The Gatas Project. Antiquity 73(282), 846–856. doi:10.1017/S0003598X00065583.

Català, A., Cacho, I., Frigola, J., Pena, L.D., Lirer, F., 2019. Holocene hydrography evolution in the Alboran Sea: A multi-record and multi-proxy comparison. Clim. Past 15(3), 927–942. doi:10.5194/cp-15-927-2019.

Chabaud, L., Sánchez Goñi, M.F., Desprat, S., Rossignol, L., 2014. Land–sea climatic variability in the eastern North Atlantic subtropical region over the last 14,200 years: Atmospheric and oceanic processes at different timescales. The Holocene 24(7), 787–797. doi:10.1177/0959683614530439.

Chapman, R., 2008. Producing Inequalities: Regional Sequences in Later Prehistoric Southern Spain. J World Prehist 21(3-4), 195–260. doi:10.1007/s10963-008-9014-y.

Cheng, H., Sinha, A., Verheyden, S., Nader, F.H., Li, X.L., Zhang, P.Z., Yin, J.J., Yi, L., Peng, Y.B., Rao, Z.G., Ning, Y.F., Edwards, R.L., 2015. The climate variability in northern Levant over the past 20,000 years. Geophysical Research Letters 42(20), 8641–8650. doi:10.1002/2015GL065397.

Clark-Carter, D., 2014. z Scores. In: Balakrishnan, N. (Ed.), Wiley StatsRef: Statistics Reference Online. Wiley, [Erscheinungsort nicht ermittelbar], p. 44.

Combourieu Nebout, N., Peyron, O., Dormoy, I., Desprat, S., Beaudouin, C., Kotthoff, U., Marret, F., 2009. Rapid climatic variability in the west Mediterranean during the last 25 000 years from high resolution pollen data. Clim. Past 5(1), 671–707. doi:10.5194/cpd-5-671-2009.

Comendador Rey, B., Millos, J., Álvarez-Iglesias, P., 2014. Provenance of the prehistoric silver set of Antas de Ulla, north-western Iberia, using lead stable isotope ratios. In: Meller, H., Risch, R., Pernicka, E. (Eds.), Metalle der Macht - frühes Gold und Silber: 6. Mitteldeutscher Archäologentag vom 17. bis 19. Oktober 2013 in Halle (Saale) = Metals of power - early gold and silver. Landesamt für Denkmalpflege und Archäologie Sachsen-Anhalt Landesmuseum für Vorgeschichte, Halle (Saale), pp. 285–308.

Contreras, D.A., Meadows, J., 2014. Summed radiocarbon calibrations as a population proxy: A critical evaluation using a realistic simulation approach. Journal of Archaeological Science 52, 591–608. doi:10.1016/j.jas.2014.05.030.

Cortés-Sánchez, M., Morales-Muñiz, A., Simón-Vallejo, M.D., Lozano-Francisco, M.C., Vera-Peláez, J.L., Finlayson, C., Rodríguez-Vidal, J., Delgado-Huertas, A., Jiménez-Espejo, F.J., Martínez-Ruiz, F., Martínez-Aguirre, M.A., Pascual-Granged, A.J., Bergadà-Zapata, M.M., Gibaja-Bao, J.F., Riquelme-Cantal, J.A., López-Sáez, J.A., Rodrigo-Gámiz, M., Sakai, S., Sugisaki, S., Finlayson, G., Fa, D.A., Bicho, N.F., 2011. Earliest known use of marine resources by Neanderthals. PloS one 6(9), e24026. doi:10.1371/journal.pone.0024026.

Crema, E.R., Bevan, A., Shennan, S., 2017. Spatio-temporal approaches to archaeological radiocarbon dates. Journal of Archaeological Science 87, 1–9. doi:10.1016/j.jas.2017.09.007.

Davis, B.A.S., Brewer, S., Stevenson, A.C., Guiot, J., 2003. The temperature of Europe during the Holocene reconstructed from pollen data. Quaternary Science Reviews 22(15-17), 1701–1716. doi:10.1016/S0277-3791(03)00173-2.

Davis, B.A.S., Stevenson, A.C., 2007. The 8.2ka event and Early–Mid Holocene forests, fires and flooding in the Central Ebro Desert, NE Spain. Quaternary Science Reviews 26(13-14), 1695–1712. doi:10.1016/j.quascirev.2007.04.007.

Delgado-Raack, S., Lull, V., Martin, K., Micó, R., Rihuete Herrada, C., Risch, R., 2014. Die Silberschmiede von Tira del Lienzo, Totana, Prov. Murcia, im Kontext der El Argar Metallurgie. In: Meller, H., Risch, R., Pernicka, E. (Eds.), Metalle der Macht - frühes Gold und Silber: 6. Mitteldeutscher Archäologentag vom 17. bis 19. Oktober 2013 in Halle (Saale) = Metals of power - early gold and silver. Landesamt für Denkmalpflege und Archäologie Sachsen-Anhalt Landesmuseum für Vorgeschichte, Halle (Saale), pp. 577–592.

Delgado-Raack, S., Risch, R., 2015. Social Change and Subsistence Production on the Iberian Peninsula during the 3rd and 2nd Millennia BCE. In: Kneisel, J., Dal Corso, M., Kirleis, W., Scholz, H., Taylor, N., Tiedtke, V. (Eds.), The Third Food Revolution?: Setting the Bronze Age table common trends in economic and subsistence strategies in Bronze Age Europe proceedings of the International Workshop "Socio-Environmental Dynamics over the Last 12,000 Years: the Creation of Landscapes III (15th-18th April 2013)" in Kiel. Verlag Dr. Rudolph Habelt GmbH, Bonn, pp. 21–46.

Díaz-Zorita Bonilla, M., 2013. The Copper Age in south-west Spain: A bioarchaeological approach to prehistoric social organisation 2013, Durham.

Díaz-Zorita Bonilla, M., Beck, J., Bocherens, H., Díaz-del-Río, P., 2018. Isotopic evidence for mobility at large-scale human aggregations in Copper Age Iberia: The mega-site of Marroquíes. Antiquity 92(364), 991–1007. doi:10.15184/aqy.2018.33.

Dorado Valiño, M., Valdeolmillos Rodríguez, A., Blanca Ruiz Zapata, M., José Gil García, M., Bustamante Gutiérrez, I. de, 2002. Climatic changes since the Late-glacial/Holocene transition in La Mancha Plain (South-central Iberian Peninsula, Spain) and their incidence on Las Tablas de Daimiel marshlands. Quaternary International 93-94, 73–84. doi:10.1016/S1040-6182(02)00007-1.

Drake, B.L., Blanco-González, A., Lillios, K.T., 2017. Regional Demographic Dynamics in the Neolithic Transition in Iberia: Results from Summed Calibrated Date Analysis. J Archaeol Method Theory 24(3), 796–812. doi:10.1007/s10816-016-9286-y.

Faust, D., Wolf, D., 2017. Interpreting drivers of change in fluvial archives of the Western Mediterranean - A critical view. Earth-Science Reviews 174, 53–83. doi:10.1016/j.earscirev.2017.09.011.

Fick, S.E., Hijmans, R.J., 2017. WorldClim 2: New 1-km spatial resolution climate surfaces for global land areas. Int. J. Climatol. 37(12), 4302–4315. doi:10.1002/joc.5086.

Fletcher, W.J., Sanchez Goñi, M.F., Peyron, O., Dormoy, I., 2010. Abrupt climate changes of the last deglaciation detected in a Western Mediterranean forest record. Clim. Past 6(2), 245–264. doi:10.5194/cp-6-245-2010.

Fletcher, W.J., Sánchez Goñi, M.F., 2008. Orbital- and sub-orbital-scale climate impacts on vegetation of the western Mediterranean basin over the last 48,000 yr. Quat. res. 70(03), 451–464. doi:10.1016/j.yqres.2008.07.002.

Franco-Múgica, F., García-Antón, M., Maldonado-Ruiz, J., Morla-Juaristi, C., Sainz-Ollero, H., 2005. Ancient pine forest on inland dunes in the Spanish northern meseta. Quat. res. 63(1), 1–14. doi:10.1016/j.yqres.2004.08.004.

Franco-Múgica, F., García-Antón, M., Maldonado-Ruiz, J., Morla-Juaristi, C., Sainz-Ollerol, H., 2001. The Holocene history of Pinus forests in the Spanish Northern Meseta. The Holocene 11(3), 343–358. doi:10.1191/095968301669474913.

Frigola, J., Moreno, A., Cacho, I., Canals, M., Sierro, F.J., Flores, J.A., Grimalt, J.O., 2008. Evidence of abrupt changes in Western Mediterranean Deep Water circulation during the last 50kyr: A high-resolution marine record from the Balearic Sea. Quaternary International 181(1), 88–104. doi:10.1016/j.quaint.2007.06.016.

Fyfe, R.M., Woodbridge, J., Palmisano, A., Bevan, A., Shennan, S., Burjachs, F., Legarra Herrero, B., García Puchol, O., Carrión, J.-S., Revelles, J., Roberts, C.N., 2019. Prehistoric palaeodemographics and regional land cover change in eastern Iberia. The Holocene 29(5), 799–815. doi:10.1177/0959683619826643.

García Sanjuán, L., Moreno Escobar, M.d.C., Márquez Pérez, J., Wheatley, D.W., 2016. The Copper Age in the lands of Antequera (Málaga): Introduction to the settlement patterns and social dynamics. Zephyrus 78, 35–65. doi:10.14201/zephyrus2016783565.

García Sanjuán, L., Scarre, C., Wheatley, D.W., 2017. The Mega-Site of Valencina de la Concepción (Seville, Spain): Debating Settlement Form, Monumentality and Aggregation in Southern Iberian Copper Age Societies. J World Prehist 30(3), 239–257. doi:10.1007/s10963-017-9107-6.

García Sanjuán, L., Vargas Jiménez, J.M., Cáceres Puro, L.M., Costa Caramé, M.E., Díaz-Guardamino Uribe, M., Díaz-Zorita Bonilla, M., Fernández Flores, Á., Hurtado Pérez, V., López Aldana, P.M., Méndez Izquierdo, E., Pajuelo Pando, A., Rodríguez Vidal, J., Wheatley, D., Bronk Ramsey, C., Delgado-Huertas, A., Dunbar, E., Mora González, A., Bayliss, A., Beavan, N., Hamilton, D., Whittle, A., 2018. Assembling the Dead, Gathering the Living: Radiocarbon Dating and Bayesian Modelling for Copper Age Valencina de la Concepción (Seville, Spain). Journal of world prehistory 31(2), 179–313. doi:10.1007/s10963-018-9114-2.

Gil García, M.J., Valiño, M.D., Rodríguez, A.V., Zapata, M.B.R., 2002. Late-glacial and Holocene palaeoclimatic record from Sierra de Cebollera (northern Iberian Range, Spain). Quaternary International 93-94, 13–18. doi:10.1016/S1040-6182(02)00003-4.

Giorgi, F., Lionello, P., 2008. Climate change projections for the Mediterranean region. Global and Planetary Change 63(2-3), 90–104. doi:10.1016/j.gloplacha.2007.09.005.

González, A.V., Saa, M.P., 2000. Analyse pollinique d'une tourbière holocène dans les Montes do Buio: Cuadramón (Galice, nord-ouest de l'Espagne) [Pollen analyse of holocene peat-bog in the Montes do Buio Cuadramón (Galice, N. W. of Spain)]. quate 11(3), 257–268. doi:10.3406/quate.2000.1674.

Gouveia, C., Trigo, R.M., DaCamara, C.C., Libonati, R., Pereira, J.M.C., 2008. The North Atlantic Oscillation and European vegetation dynamics. Int. J. Climatol. 28(14), 1835–1847. doi:10.1002/joc.1682.

Haynes, R., Barton, E.D., Pilling, I., 1993. Development, persistence, and variability of upwelling filaments off the Atlantic coast of the Iberian Peninsula. J. Geophys. Res. 98(C12), 22681. doi:10.1029/93JC02016.

Hernández, A., Trigo, R.M., Pla-Rabes, S., Valero-Garcés, B.L., Jerez, S., Rico-Herrero, M., Vega, J.C., Jambrina-Enríquez, M., Giralt, S., 2015. Sensitivity of two Iberian lakes to North Atlantic atmospheric circulation modes. Clim Dyn 45(11-12), 3403–3417. doi:10.1007/s00382-015-2547-8.

Hijmans, R.J., 2019. raster: Geographic Data Analysis and Modeling.

Hinz, M., Feeser, I., Sjögren, K.-G., Müller, J., 2012a. Demography and the intensity of cultural activities: An evaluation of Funnel Beaker Societies (4200–2800 cal BC). Journal of Archaeological Science 39(10), 3331–3340. doi:10.1016/j.jas.2012.05.028.

Hinz, M., Furholt, M., Müller, J., Raetzel-Fabian, D., Rinne, C., Sjögren, K.-G., Wotza, H.-P., 2012b. RADON - Radiocarbon dates online 2012: Central European database of 14C dates for the Neolithic and Early Bronze Age. www.jungsteinsite.de.

Hinz, M., Schirrmacher, J., Kneisel, J., Rinne, C., Weinelt, M., 2019. The Chalcolithic–Bronze Age transition in southern Iberia under the influence of the 4.2 kyr event?: A correlation of climatological and demographic proxies. Journal of Neolithic Archaeology 21, 1–26. doi:10.12766/jna.2019.1.

Hurrell, J.W., 1995. Decadal trends in the north atlantic oscillation: regional temperatures and precipitation. Science 269(5224), 676–679. doi:10.1126/science.269.5224.676.

IDEArq (n.d.). IDEArq: Infraestructura de Datos Espaciales de Investigación Arqueológica. http://www.idearqueologia.org/.

Ilvonen, L., López-Sáez, J.A., Holmström, L., Alba-Sánchez, F., Pérez-Díaz, S., Carrión, J.S., Seppä, H., 2019. Quantitative reconstruction of precipitation changes in the Iberian Peninsula during the Late Pleistocene and the Holocene. Clim. Past Discuss., 1–30. doi:10.5194/cp-2019-33.

Jalali, B., Sicre, M.-A., Bassetti, M.-A., Kallel, N., 2016. Holocene climate variability in the North-Western Mediterranean Sea (Gulf of Lions). Climate of the Past 12(1), 91–101. doi:10.5194/cp-12-91-2016.
Jalut, G., Dedoubat, J.J., Fontugne, M., Otto, T., 2009. Holocene circum-Mediterranean vegetation changes: Climate forcing and human impact. Quaternary International 200(1-2), 4–18. doi:10.1016/j.quaint.2008.03.012.
Jiménez-Moreno, G., Anderson, R.S., 2012. Holocene vegetation and climate change recorded in alpine bog sediments from the Borreguiles de la Virgen, Sierra Nevada, southern Spain. Quat. res. 77(01), 44–53. doi:10.1016/j.yqres.2011.09.006.
Jiménez-Moreno, G., Rodríguez-Ramírez, A., Pérez-Asensio, J.N., Carrión, J.S., López-Sáez, J.A., Villarías-Robles, J., JR, Celestino-Pérez, S., Cerrillo-Cuenca, E., León, Á., Contreras, C., 2015. Impact of late-Holocene aridification trend, climate variability and geodynamic control on the environment from a coastal area in SW Spain. The Holocene 25(4), 607–617. doi:10.1177/0959683614565955.
Jones, S.E., Burjachs, F., Ferrer-García, C., Giralt, S., Schulte, L., Fernández-López de Pablo, J., 2018. A multi-proxy approach to understanding complex responses of salt-lake catchments to climate variability and human pressure: A Late Quaternary case study from south-eastern, Spain. Quaternary Science Reviews 184, 201–223. doi:10.1016/j.quascirev.2017.12.015.
Kaniewski, D., Marriner, N., Cheddadi, R., Guiot, J., van Campo, E., 2018. The 4.2 ka BP event in the Levant. Clim. Past 14(10), 1529–1542. doi:10.5194/cp-14-1529-2018.
Kim, J.-H., Schouten, S., Rodrigo-Gámiz, M., Rampen, S., Marino, G., Huguet, C., Helmke, P., Buscail, R., Hopmans, E.C., Pross, J., Sangiorgi, F., Middelburg, J.B.M., Sinninghe Damsté, J.S., 2015. Influence of deep-water derived isoprenoid tetraether lipids on the TEX86H paleothermometer in the Mediterranean Sea. Geochimica et Cosmochimica Acta 150, 125–141. doi:10.1016/j.gca.2014.11.017.
Kneisel, J., Hinz, M., Rinne, C., 2013. Radon-B. http://radon-b.ufg.uni-kiel.de.
Kovats, R.S., Valentini, R., Bouwer, L.M., Georgopoulou, E., Jacob, D., Martin, E., Rounsevell, M., Soussana, J.-F., 2014. Europe. In: Barros, V.R., Field, C.B., Dokken, D.J., Mastrandrea, M.D., Mach, K.J., Bilir, T.E., Chatterjee, M., Ebi, K.L., Estrada, Y.O., Genova, R.C., Girma, B., Kissel, E.S., Levy, A.N., MacCracken, S., Mastrandrea, P.R., White, L.L. (Eds.), Climate Change 2014: Impacts, Adaptation, and Vulnerability. Part B: Regional Aspects.Contribution of Working Group II to the Fifth Assessment Report of the Intergovernmental Panel on Climate Change, Cambridge, United Kingdom and New York, NY, USA, pp. 1267–1326.
Kunst, M., Lutz, N., 2008. Zambujal (Torres Vedras, Portugal): Zur Präzision der absoluten Chronologie durch die Untersuchungen an der vierten Befestigungslinie. In: Deutsches Archäologisches Institut (Ed.), Madrider Mitteilungen. Ludwig Reichert Verlag, Wiesbaden, pp. 29–63.
Lamb, H.F., van der Kaars, S., 1995. Vegetational response to Holocene climatic change: Pollen and palaeolimnological data from the Middle Atlas, Morocco. The Holocene 5(4), 400–408. doi:10.1177/095968369500500402.
Lillios, K.T., Blanco-González, A., Drake, B.L., López-Sáez, J.A., 2016. Mid-late Holocene climate, demography, and cultural dynamics in Iberia: A multi-proxy approach. Quaternary Science Reviews 135, 138–153. doi:10.1016/j.quascirev.2016.01.011.
Lionello, P. (Ed.), 2012. The climate of the Mediterranean region: From the past to the future, 1. ed. ed. Elsevier insights. Elsevier Science, Amsterdam.
López Saez, J.A., Blanco González, A., Pérez Díaz, S., Alba Sánchez, F., Luelmo Lautenschlaeger, R., Glais, A., Núñez de la Fuente, S., 2017. Landscapes, Human Activities and Climate Dynamics in the South Meseta of the Iberian Peninsula During the 3rd and 2nd Millennia calBC. In: Bartelheim, M., Bueno Ramírez, P., Kunst, M. (Eds.), Key resources and socio-cultural developments in the Iberian Chalcolithic. Eberhard Karls Universität Tübingen Tübingen Library Publishing, Tübingen, pp. 129–142.

López-Merino, L., Cortizas, A.M., López-Sáez, J.A., 2010. Early agriculture and palaeoenvironmental history in the North of the Iberian Peninsula: A multi-proxy analysis of the Monte Areo mire (Asturias, Spain). Journal of Archaeological Science 37(8), 1978–1988. doi:10.1016/j.jas.2010.03.003.
López-Merino, L., Silva Sánchez, N., Kaal, J., López-Sáez, J.A., Martínez Cortizas, A., 2012. Post-disturbance vegetation dynamics during the Late Pleistocene and the Holocene: An example from NW Iberia. Global and Planetary Change 92-93, 58–70. doi:10.1016/j.gloplacha.2012.04.003.
López-Sáez, J.A., Abel-Schaad, D., Pérez-Díaz, S., Blanco-González, A., Alba-Sánchez, F., Dorado, M., Ruiz-Zapata, B., Gil-García, M.J., Gómez-González, C., Franco-Múgica, F., 2014. Vegetation history, climate and human impact in the Spanish Central System over the last 9000 years. Quaternary International 353, 98–122. doi:10.1016/j.quaint.2013.06.034.
López-Sáez, J.A., Pérez-Díaz, S., Rodríguez-Ramírez, A., Blanco-González, A., Villarías-Robles, J.J.R., Luelmo-Lautenschlaeger, R., Jiménez-Moreno, G., Celestino-Pérez, S., Cerrillo-Cuenca, E., Pérez-Asensio, J.N., León, Á., 2018. Mid-late Holocene environmental and cultural dynamics at the south-west tip of Europe (Doñana National Park, SW Iberia, Spain). Journal of Archaeological Science: Reports 22, 58–78. doi:10.1016/j.jasrep.2018.09.014.
Lull, V., Micó, R., Rihuete Herrada, C., Risch, R., 2011. El Argar and the Beginning of Class Society in the Western Mediterranean. In: Hansen, S., Müller, J. (Eds.), Sozialarchäologische Perspektiven: Gesellschaftlicher Wandel 5000 - 1500 v. Chr. zwischen Atlantik und Kaukasus: Internationale Tagung, 15. - 18. Oktober 2007 in Kiel. von Zabern, Mainz, pp. 381–414.
Lull, V., Micó, R., Rihuete Herrada, C., Risch, R., 2013a. Bronze Age Iberia. In: Fokkens, H., Harding, A. (Eds.), The Oxford Handbook of the European Bronze Age. Oxford University Press.
Lull, V., Micó, R., Rihuete Herrada, C., Risch, R., 2013b. Political collapse and social change at the end of El Argar. In: Meller, H., Bertemes, F., Bork, H.-R., Risch, R. (Eds.), 1600 - Kultureller Umbruch im Schatten des Thera-Ausbruchs?: 4. Mitteldeutscher Archäologentag vom 14. bis 16. Oktober 2011 in Halle (Saale). Landesamt für Denkmalpflege und Archäologie Sachsen-Anhalt, Landesmuseum für Vorgeschichte, Halle (Saale), pp. 283–302.
Lull, V., Micó, R., Rihuete Herrada, C., Risch, R., 2015. Transition and conflict at the end of the 3rd millennium BC in south Iberia. In: Meller, H., Arz, H.W., Jung, R., Risch, R. (Eds.), 2200 BC - ein Klimasturz als Ursache für den Zerfall der alten Welt?: 7. Mitteldeutscher Archäologentag vom 23. bis 26. Oktober 2014 in Halle (Saale). Landesamt für Denkmalpflege und Archäologie Sachsen-Anhalt, Landesmuseum für Vorgeschichte, Halle (Saale), pp. 365–408.
Mariscal, B., 1993. Variacion de la Vegetation Holocena (4300-280 B.P.): De Cantabria a traves del analisis polinico de la Turbera del Alsa. Estud. geol. 49(1-2), 63–68. doi:10.3989/egeol.93491-2338.
Mariscal Álvarez, B., 1983. Estudio polínico de la turbera del Cueto de la Avellanosa, Polaciones (Cantabria). Series Cadernos do Laboratorio de Laxe 5, 205–226.
Martín-Chivelet, J., Muñoz-García, M.B., Edwards, R.L., Turrero, M.J., Ortega, A.I., 2011. Land surface temperature changes in Northern Iberia since 4000yrBP, based on δ13C of speleothems. Global and Planetary Change 77(1-2), 1–12. doi:10.1016/j.gloplacha.2011.02.002.
Martrat, B., Grimalt, J.O., Shackleton, N.J., Abreu, L. de, Hutterli, M.A., Stocker, T.F., 2007. Four climate cycles of recurring deep and surface water destabilizations on the Iberian margin. Science (New York, N.Y.) 317(5837), 502–507. doi:10.1126/science.1139994.
Mary, Y., Eynaud, F., Colin, C., Rossignol, L., Brocheray, S., Mojtahid, M., Garcia, J., Peral, M., Howa, H., Zaragosi, S., Cremer, M., 2017. Changes in Holocene meridional circulation and poleward Atlantic flow: The Bay of Biscay as a nodal point. Climate of the Past 13(3), 201–216. doi:10.5194/cp-13-201-2017.
McDermott, F., Frisia, S., Huang, Y., Longinelli, A., Spiro, B., Heaton, T.H.E., Hawkesworth, C.J., Borsato, A., Keppens, E., Fairchild, I.J., van der Borg, K., Verheyden, S., Selmo, E., 1999. Holocene climate variability in Europe: Evidence from δ18O, textural and extension-rate variations in three speleothems. Quaternary Science Reviews 18(8), 1021–1038. doi:10.1016/S0277-3791(98)00107-3.

Mesa-Fernández, J.M., Jiménez-Moreno, G., Rodrigo-Gámiz, M., García-Alix, A., Jiménez-Espejo, F.J., Martínez-Ruiz, F., Anderson, R.S., Camuera, J., Ramos-Román, M.J., 2018. Vegetation and geochemical responses to Holocene rapid climate change in the Sierra Nevada (southeastern Iberia): The Laguna Hondera record. Clim. Past 14(11), 1687–1706. doi:10.5194/cp-14-1687-2018.
Molina González, F., Camara Serrano, J.A., Capel Martínez, J., Nájera Colino, T., Sáez Pérez, L., 2004. Los Millares y la periodización de la prehistoria reciente del sureste. In: Pellicer Catalán, M., Arribas, A. (Eds.), II -III Simposios de prehistoria Cueva de Nerja. Fundación Cueva de Nerja, Nerja, pp. 142–158.
Mora-González, A., Delgado-Huertas, A., Granados-Torres, A., Contreras Cortés, F., Jover Maestre, F.J., López Padilla, J.A., 2016. The isotopic footprint of irrigation in the western Mediterranean basin during the Bronze Age: The settlement of Terlinques, southeast Iberian Peninsula. Veget Hist Archaeobot 25(5), 459–468. doi:10.1007/s00334-016-0560-4.
Mora-González, A., Delgado-Huertas, A., Granados-Torres, A., Contreras Cortés, F., Pavón Soldevila, I., Duque Espino, D., 2018. Complex agriculture during the second millennium BC: Isotope composition of carbon studies (δ13C) in archaeological plants of the settlement Cerro del Castillo de Alange (SW Iberian Peninsula, Spain). Veget Hist Archaeobot 27(3), 453-462. doi:10.1007/s00334-017-0634-y.
Morales-Molino, C., García-Antón, M., Postigo-Mijarra, J.M., Morla, C., 2013. Holocene vegetation, fire and climate interactions on the westernmost fringe of the Mediterranean Basin. Quaternary Science Reviews 59, 5–17. doi:10.1016/j.quascirev.2012.10.027.
Morales-Molino, C., Tinner, W., García-Antón, M., Colombaroli, D., McGlone, M., 2017. The historical demise of Pinus nigra forests in the Northern Iberian Plateau (south-western Europe). J Ecol 105(3), 634–646. doi:10.1111/1365-2745.12702.
Morellón, M., Valero-Garcés, B., Vegas-Vilarrúbia, T., González-Sampériz, P., Romero, Ó., Delgado-Huertas, A., Mata, P., Moreno, A., Rico, M., Corella, J.P., 2009. Lateglacial and Holocene palaeohydrology in the western Mediterranean region: The Lake Estanya record (NE Spain). Quaternary Science Reviews 28(25-26), 2582–2599. doi:10.1016/j.quascirev.2009.05.014.
Moreno, A., Pérez-Mejías, C., Bartolomé, M., Sancho, C., Cacho, I., Stoll, H., Delgado-Huertas, A., Hellstrom, J., Edwards, R.L., Cheng, H., 2017. New speleothem data from Molinos and Ejulve caves reveal Holocene hydrological variability in northeast Iberia. Quat. res. 88(02), 223–233. doi:10.1017/qua.2017.39.
Müller, J., van Willigen, S., 2001. New radiocarbon evidence for european Bell Beakers and the consequences for the diffusion of the Bell Beaker Phenomenon. In: Nicolis, F. (Ed.), Bell beakers today: Pottery, people, culture, symbols in prehistoric Europe ; proceedings of the International colloquium, Riva del Garda (Trento, Italy), 11-16 May 1998. Provincia autonoma di Trento Servizio beni culturali Ufficio beni archeologici, Trento, pp. 59–80.
Muñoz, A., Bartolomé, M., Muñoz, A., Sancho, C., Moreno, A., Hellstrom, J.C., Osácar, M.C., Cacho, I., 2015. Solar influence and hydrological variability during the Holocene from a speleothem annual record (Molinos Cave, NE Spain). Terra Nova 27(4), 300–311. doi:10.1111/ter.12160.
Palumbo, E., Flores, J.A., Perugia, C., Emanuele, D., Petrillo, Z., Rodrigues, T., Voelker, A.H.L., Amore, F.O., 2013. Abrupt variability of the last 24 ka BP recorded by coccolithophore assemblages off the Iberian Margin (core MD03-2699). J. Quaternary Sci. 28(3), 320–328. doi:10.1002/jqs.2623.
Pantaléon-Cano, J., Yll, E.-I., Pérez-Obiol, R., Roure, J.M., 2003. Palynological evidence for vegetational history in semi-arid areas of the western Mediterranean (Almería, Spain). The Holocene 13(1), 109–119. doi:10.1191/0959683603hl598rp.
Pebesma, E.J., 2004. Multivariable geostatistics in S: The gstat package. Computers & Geosciences 30(7), 683–691. doi:10.1016/j.cageo.2004.03.012.
Peliz, Á., Dubert, J., Santos, A.M.P., Oliveira, P.B., Le Cann, B., 2005. Winter upper ocean circulation in the Western Iberian Basin—Fronts, Eddies and Poleward Flows: An overview. Deep Sea Research Part I: Oceanographic Research Papers 52(4), 621–646. doi:10.1016/j.dsr.2004.11.005.

Peliz, Á., Rosa, T.L., Santos, A.M.P., Pissarra, J.L., 2002. Fronts, jets, and counter-flows in the Western Iberian upwelling system. Journal of Marine Systems 35(1-2), 61–77. doi:10.1016/S0924-7963(02)00076-3.

Pérez-Obiol, R., Jalut, G., Julià, R., Pèlachs, A., Iriarte, M.J., Otto, T., Hernández-Beloqui, B., 2011. Mid-Holocene vegetation and climatic history of the Iberian Peninsula. The Holocene 21(1), 75–93. doi:10.1177/0959683610384161.

Pérez-Sanz, A., González-Sampériz, P., Moreno, A., Valero-Garcés, B., Gil-Romera, G., Rieradevall, M., Tarrats, P., Lasheras-Álvarez, L., Morellón, M., Belmonte, A., Sancho, C., Sevilla-Callejo, M., Navas, A., 2013. Holocene climate variability, vegetation dynamics and fire regime in the central Pyrenees: The Basa de la Mora sequence (NE Spain). Quaternary Science Reviews 73, 149–169. doi:10.1016/j.quascirev.2013.05.010.

Peyron, O., Combourieu-Nebout, N., Brayshaw, D., Goring, S., Andrieu-Ponel, V., Desprat, S., Fletcher, W., Gambin, B., Ioakim, C., Joannin, S., Kotthoff, U., Kouli, K., Montade, V., Pross, J., Sadori, L., Magny, M., 2017. Precipitation changes in the Mediterranean basin during the Holocene from terrestrial and marine pollen records: A model–data comparison. Climate of the Past 13(3), 249–265. doi:10.5194/cp-13-249-2017.

R Core Team, 2019. R: A Language and Environment for Statistical Computing. R Foundation for Statistical Computing, Vienna, Austria.

Railsback, L.B., Liang, F., Vidal Romaní, J.R., Grandal-d'Anglade, A., Vaqueiro Rodríguez, M., Santos Fidalgo, L., Fernández Mosquera, D., Cheng, H., Edwards, R.L., 2011. Petrographic and isotopic evidence for Holocene long-term climate change and shorter-term environmental shifts from a stalagmite from the Serra do Courel of northwestern Spain, and implications for climatic history across Europe and the Mediterranean. Palaeogeography, Palaeoclimatology, Palaeoecology 305(1-4), 172–184. doi:10.1016/j.palaeo.2011.02.030.

Ramos-Román, M.J., Jiménez-Moreno, G., Camuera, J., García-Alix, A., Scott Anderson, R., Jiménez-Espejo, F.J., Sachse, D., Toney, J.L., Carrión, J.S., Webster, C., Yanes, Y., 2018. Millennial-scale cyclical environment and climate variability during the Holocene in the western Mediterranean region deduced from a new multi-proxy analysis from the Padul record (Sierra Nevada, Spain). Global and Planetary Change 168, 35–53. doi:10.1016/j.gloplacha.2018.06.003.

Reimer, P.J., Bard, E., Bayliss, A., Beck, J.W., Blackwell, P.G., Ramsey, C.B., Buck, C.E., Cheng, H., Edwards, R.L., Friedrich, M., Grootes, P.M., Guilderson, T.P., Haflidason, H., Hajdas, I., Hatté, C., Heaton, T.J., Hoffmann, D.L., Hogg, A.G., Hughen, K.A., Kaiser, K.F., Kromer, B., Manning, S.W., Niu, M., Reimer, R.W., Richards, D.A., Scott, E.M., Southon, J.R., Staff, R.A., Turney, C.S.M., van der Plicht, J., 2013. IntCal13 and Marine13 Radiocarbon Age Calibration Curves 0–50,000 Years cal BP. Radiocarbon 55(04), 1869–1887. doi:10.2458/azu_js_rc.55.16947.

Rodrigo-Gámiz, M., Martínez-Ruiz, F., Rampen, S.W., Schouten, S., Sinninghe Damsté, J.S., 2014. Sea surface temperature variations in the western Mediterranean Sea over the last 20 kyr: A dual-organic proxy (U K′37 and LDI) approach. Paleoceanography 29(2), 87–98. doi:10.1002/2013PA002466.

Rodrigues, T., Grimalt, J.O., Abrantes, F., Naughton, F., Flores, J.-A., 2010. The last glacial–interglacial transition (LGIT) in the western mid-latitudes of the North Atlantic: Abrupt sea surface temperature change and sea level implications. Quaternary Science Reviews 29(15-16), 1853–1862. doi:10.1016/j.quascirev.2010.04.004.

Rodrigues, T., Grimalt, J.O., Abrantes, F.G., Flores, J.A., Lebreiro, S.M., 2009. Holocene interdependences of changes in sea surface temperature, productivity, and fluvial inputs in the Iberian continental shelf (Tagus mud patch). Geochemistry, Geophysics, Geosystems 10(7), n/a-n/a. doi:10.1029/2008GC002367.

Ruan, J., Kherbouche, F., Genty, D., Blamart, D., Cheng, H., Dewilde, F., Hachi, S., Edwards, R.L., Régnier, E., Michelot, J.-L., 2016. Evidence of a prolonged drought ca. 4200 yr BP correlated with prehistoric settlement abandonment from the Gueldaman GLD1 Cave, Northern Algeria. Climate of the Past 12(1), 1–14. doi:10.5194/cp-12-1-2016.

Sabatier, P., Dezileau, L., Colin, C., Briqueu, L., Bouchette, F., Martinez, P., Siani, G., Raynal, O., Grafenstein, U. von, 2012. 7000 years of paleostorm activity in the NW Mediterranean Sea in response to Holocene climate events. Quat. res. 77(01), 1–11. doi:10.1016/j.yqres.2011.09.002.
Salgueiro, E., Naughton, F., Voelker, A.H.L., Abreu, L. de, Alberto, A., Rossignol, L., Duprat, J., Magalhães, V.H., Vaqueiro, S., Turon, J.-L., Abrantes, F., 2014. Past circulation along the western Iberian margin: A time slice vision from the Last Glacial to the Holocene. Quaternary Science Reviews 106, 316–329. doi:10.1016/j.quascirev.2014.09.001.
Sánchez Goñi, M.F., Hannon, G.E., 1999. High-altitude vegetational pattern on the Iberian Mountain Chain (north-central Spain) during the Holocene. The Holocene 9(1), 39–57.
Santos, L., Sánchez Goñi, M.F., 2003. Lateglacial and Holocene environmental changes in Portuguese coastal lagoons 3: Vegetation history of the Santo Andre coastal area. The Holocene 13(3), 459–464. doi:10.1191/0959683603hl638rp.
Sarhan, T., Lafuente, J.G., Vargas, M., Vargas, J.M., Plaza, F., 2000. Upwelling mechanisms in the northwestern Alboran Sea. Journal of Marine Systems 23(4), 317–331. doi:10.1016/S0924-7963(99)00068-8.
Schirrmacher, J., Weinelt, M., Blanz, T., Andersen, N., Salgueiro, E., Schneider, R.R., 2019. Multi-decadal atmospheric and marine climate variability in southern Iberia during the mid- to late-Holocene. Clim. Past 15(2), 617–634. doi:10.5194/cp-15-617-2019.
Schneider, H., Höfer, D., Trog, C., Busch, S., Schneider, M., Baade, J., Daut, G., Mäusbacher, R., 2010. Holocene estuary development in the Algarve Region (Southern Portugal) – A reconstruction of sedimentological and ecological evolution. Quaternary International 221(1-2), 141–158. doi:10.1016/j.quaint.2009.10.004.
Schneider, H., Höfer, D., Trog, C., Mäusbacher, R., 2016. Holocene landscape development along the Portuguese Algarve coast – A high resolution palynological approach. Quaternary International 407, 47–63. doi:10.1016/j.quaint.2016.02.039.
Schröder, T., van‘t Hoff, J., López-Sáez, J.A., Viehberg, F., Melles, M., Reicherter, K., 2018. Holocene climatic and environmental evolution on the southwestern Iberian Peninsula: A high-resolution multi-proxy study from Lake Medina (Cádiz, SW Spain). Quaternary Science Reviews 198, 208–225. doi:10.1016/j.quascirev.2018.08.030.
Schuhmacher, T.X., 2017. Ivory Exchange Networks in the Chalcolithic of the Western Mediterranean. In: Bartelheim, M., Bueno Ramírez, P., Kunst, M. (Eds.), Key resources and socio-cultural developments in the Iberian Chalcolithic. Eberhard Karls Universität Tübingen Tübingen Library Publishing, Tübingen, pp. 291–312.
Schulz Paulsson, B., 2019. Radiocarbon dates and Bayesian modeling support maritime diffusion model for megaliths in Europe. Proceedings of the National Academy of Sciences of the United States of America 116(9), 3460–3465. doi:10.1073/pnas.1813268116.
Smith, A.C., Wynn, P.M., Barker, P.A., Leng, M.J., Noble, S.R., Tych, W., 2016. North Atlantic forcing of moisture delivery to Europe throughout the Holocene. Scientific reports 6, 24745. doi:10.1038/srep24745.
Soares, A.M.M., Soares, J., Tavares da Silva, C., 2007. A datação pelo radiocarbono das fases de ocupação do Porto das Carretas: algumas reflexões sobre a cronologia do Campaniforme. Revista Portuguesa de Arqueologia 10(2), 127–134.
Stefanini, B.S., Oksanen, P.O., Corcoran, J.P., Mitchell, F.J.G., 2018. Appraising the cohesion of palaeoenvironmental reconstructions in north-west Spain since the mid-Holocene from a high temporal resolution multi-proxy peat record. The Holocene 28(5), 681–694. doi:10.1177/0959683617744258.
Tarrats, P., Heiri, O., Valero-Garcés, B., Cañedo-Argüelles, M., Prat, N., Rieradevall, M., González-Sampériz, P., 2018. Chironomid-inferred Holocene temperature reconstruction in Basa de la Mora Lake (Central Pyrenees). The Holocene 28(11), 1685–1696. doi:10.1177/0959683618788662.
Trigo, R.M., Pozo-Vázquez, D., Osborn, T.J., Castro-Díez, Y., Gámiz-Fortis, S., Esteban-Parra, M.J., 2004. North Atlantic oscillation influence on precipitation, river flow and water resources in the Iberian Peninsula. Int. J. Climatol 24(8), 925–944. doi:10.1002/joc.1048.

Trog, C., Höfer, D., Frenzel, P., Camacho, S., Schneider, H., Mäusbacher, R., 2013. A multi-proxy reconstruction and comparison of Holocene palaeoenvironmental changes in the Alvor and Alcantarilha estuaries (southern Portugal). Revue de Micropaléontologie 56(4), 131–158. doi:10.1016/j.revmic.2013.10.003.

Valera, A.C., 2015. Social change in the late 3rd millennium BC in Portugal: the twilight of enclosures. In: Meller, H., Arz, H.W., Jung, R., Risch, R. (Eds.), 2200 BC - ein Klimasturz als Ursache für den Zerfall der alten Welt?: 7. Mitteldeutscher Archäologentag vom 23. bis 26. Oktober 2014 in Halle (Saale). Landesamt für Denkmalpflege und Archäologie Sachsen-Anhalt, Landesmuseum für Vorgeschichte, Halle (Saale), pp. 409–428.

van den Brink, L.M., Janssen, C.R., 1985. The effect of human activities during cultural phases on the development of montane vegetation in the Serra de Estrela, Portugal. Review of Palaeobotany and Palynology 44(3-4), 193–215. doi:10.1016/0034-6667(85)90016-8.

van der Knaap, W.O., van Leeuwen, J.F.N., 1995. Holocene vegetation succession and degradation as responses to climatic change and human activity in the Serra de Estrela, Portugal. Review of Palaeobotany and Palynology 89(3-4), 153–211. doi:10.1016/0034-6667(95)00048-0.

Vis, G.-J., Bohncke, S.J.P., Schneider, H., Kasse, C., Coenraads-Nederveen, S., Zuurbier, K., Rozema, J., 2010. Holocene flooding history of the Lower Tagus Valley (Portugal). J. Quaternary Sci. 25(8), 1222–1238. doi:10.1002/jqs.1401.

Walczak, I.W., Baldini, J.U.L., Baldini, L.M., McDermott, F., Marsden, S., Standish, C.D., Richards, D.A., Andreo, B., Slater, J., 2015. Reconstructing high-resolution climate using CT scanning of unsectioned stalagmites: A case study identifying the mid-Holocene onset of the Mediterranean climate in southern Iberia. Quaternary Science Reviews 127, 117–128. doi:10.1016/j.quascirev.2015.06.013.

Walsh, K., Berger, J.-F., Roberts, C.N., Vanniere, B., Ghilardi, M., Brown, A.G., Woodbridge, J., Lespez, L., Estrany, J., Glais, A., Palmisano, A., Finné, M., Verstraeten, G., 2019. Holocene demographic fluctuations, climate and erosion in the Mediterranean: A meta data-analysis. The Holocene 29(5), 864–885. doi:10.1177/0959683619826637.

Warden, L., Moros, M., Neumann, T., Shennan, S., Timpson, A., Manning, K., Sollai, M., Wacker, L., Perner, K., Häusler, K., Leipe, T., Zillén, L., Kotilainen, A., Jansen, E., Schneider, R.R., Oeberst, R., Arz, H., Sinninghe Damsté, J.S., 2017. Climate induced human demographic and cultural change in northern Europe during the mid-Holocene. Scientific reports 7(1), 15251. doi:10.1038/s41598-017-14353-5.

Wassenburg, J.A., Dietrich, S., Fietzke, J., Fohlmeister, J., Jochum, K.P., Scholz, D., Richter, D.K., Sabaoui, A., Spötl, C., Lohmann, G., Andreae, M.O., Immenhauser, A., 2016. Reorganization of the North Atlantic Oscillation during early Holocene deglaciation. Nature Geoscience 9(8), 602–605. doi:10.1038/ngeo2767.

Weinelt, M., Schwab, C., Kneisel, J., Hinz, M., 2015. Climate and societal change in the western Mediterranean area around 4.2 ka BP. In: Meller, H., Arz, H.W., Jung, R., Risch, R. (Eds.), 2200 BC - ein Klimasturz als Ursache für den Zerfall der alten Welt?: 7. Mitteldeutscher Archäologentag vom 23. bis 26. Oktober 2014 in Halle (Saale). Landesamt für Denkmalpflege und Archäologie Sachsen-Anhalt, Landesmuseum für Vorgeschichte, Halle (Saale), pp. 461–480.

Weiss, H., 2017. 4.2 ka BP Megadrought and the Akkadian Collapse. In: Weiss, H. (Ed.), Megadrought and collapse: From early agriculture to angkor. Oxford University Press, New York, NY, pp. 93–161.

Welc, F., Marks, L., 2014. Climate change at the end of the Old Kingdom in Egypt around 4200 BP: New geoarchaeological evidence. Quaternary International 324, 124–133. doi:10.1016/j.quaint.2013.07.035.

Weninger, B., Clare, L., Jöris, O., Jung, R., Edinborough, K., 2015. Quantum theory of radiocarbon calibration. World Archaeology 47(4), 543–566. doi:10.1080/00438243.2015.1064022.

Williams, A.N., 2012. The use of summed radiocarbon probability distributions in archaeology: A review of methods. Journal of Archaeological Science 39(3), 578–589. doi:10.1016/j.jas.2011.07.014.

Yll, E.-I., Perez-Obiol, R., Pantaleon-Cano, J., Roure, J.M., 1997. Palynological Evidence for Climatic Change and Human Activity during the Holocene on Minorca (Balearic Islands). Quat. res. 48(03), 339–347. doi:10.1006/qres.1997.1925.

Zanchetta, G., Regattieri, E., Isola, I., Drysdale, R.N., Bini, M., Baneschi, I., Hellstrom, J.C., 2016. The so-called "4.2 event" in the Central Mediterranean and its climatic teleconnections. Alpine and Mediterranean Quaternary 29(1), 5–17.

Zielhofer, C., Fletcher, W.J., Mischke, S., Batist, M. de, Campbell, J.F.E., Joannin, S., Tjallingii, R., El Hamouti, N., Junginger, A., Stele, A., Bussmann, J., Schneider, B., Lauer, T., Spitzer, K., Strupler, M., Brachert, T., Mikdad, A., 2017. Atlantic forcing of Western Mediterranean winter rain minima during the last 12,000 years. Quaternary Science Reviews 157, 29–51. doi:10.1016/j.quascirev.2016.11.037.

Zielhofer, C., Köhler, A., Mischke, S., Benkaddour, A., Mikdad, A., Fletcher, W.J., 2019. Western Mediterranean hydro-climatic consequences of Holocene ice-rafted debris (Bond) events. Clim. Past 15(2), 463–475. doi:10.5194/cp-15-463-2019.

Zorita, E., Kharin, V., Storch, H. von, 1992. The Atmospheric Circulation and Sea Surface Temperature in the North Atlantic Area in Winter: Their Interaction and Relevance for Iberian Precipitation. Journal of Climate 5(10), 1097–1108. doi:10.1175/1520-0442(1992)005<1097:TACASS>2.0.CO;2.

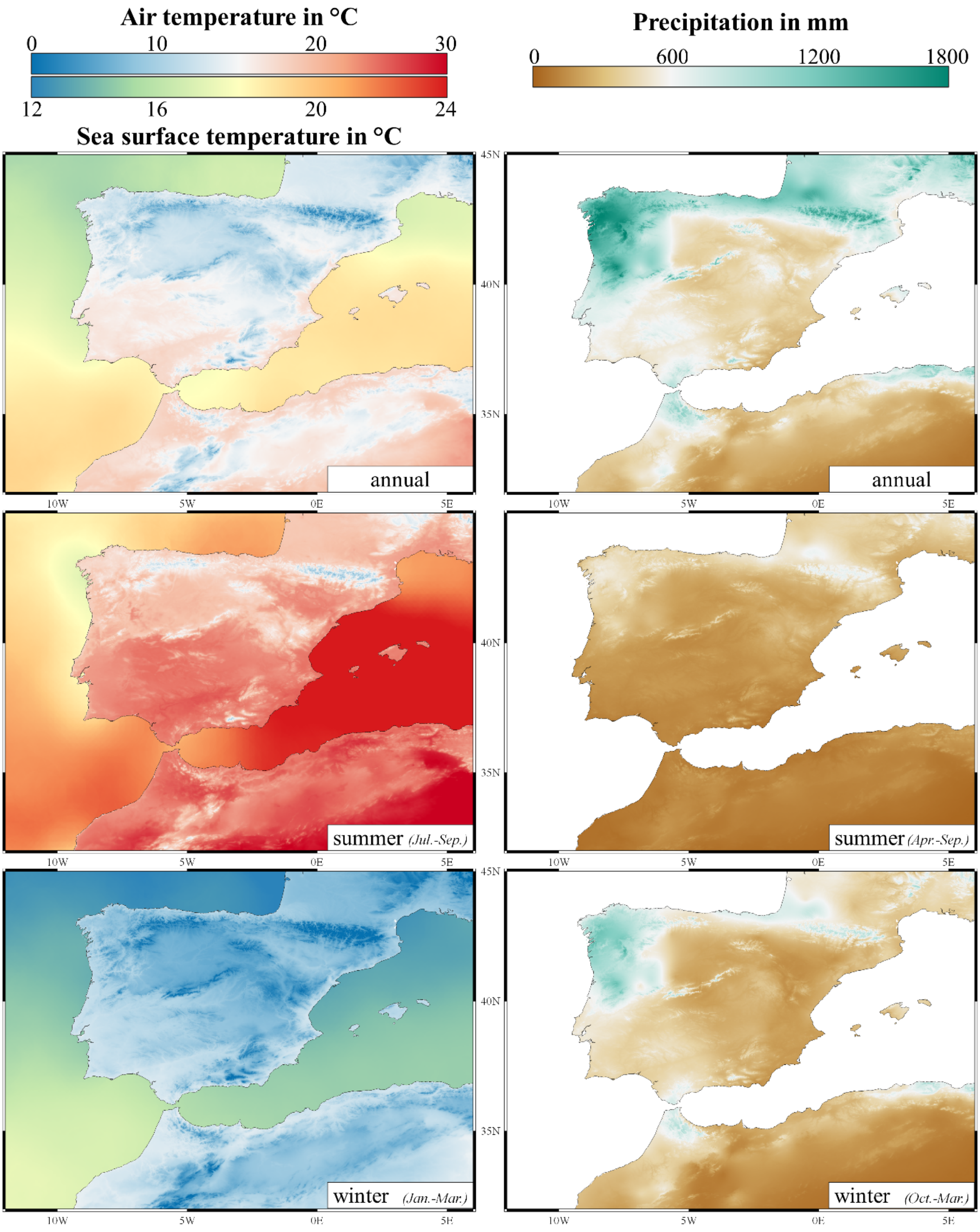

Fig. S1. Recent annual and seasonal air temperature as well as sea surface temperature (left) and precipitation (right) at the Iberian Peninsula. Temperatures are averages, while precipitation is displayed as total amount. Precipitation and air temperatures are based on monthly averages (1970 – 2000) and were downloaded from WorldClim V2 (Fick and Hijmans, 2017). Sea surface temperature data are averaged for the period from 1955 – 2017 and was provided by World Ocean Atlas 18 (Locarnini et al., 2019).

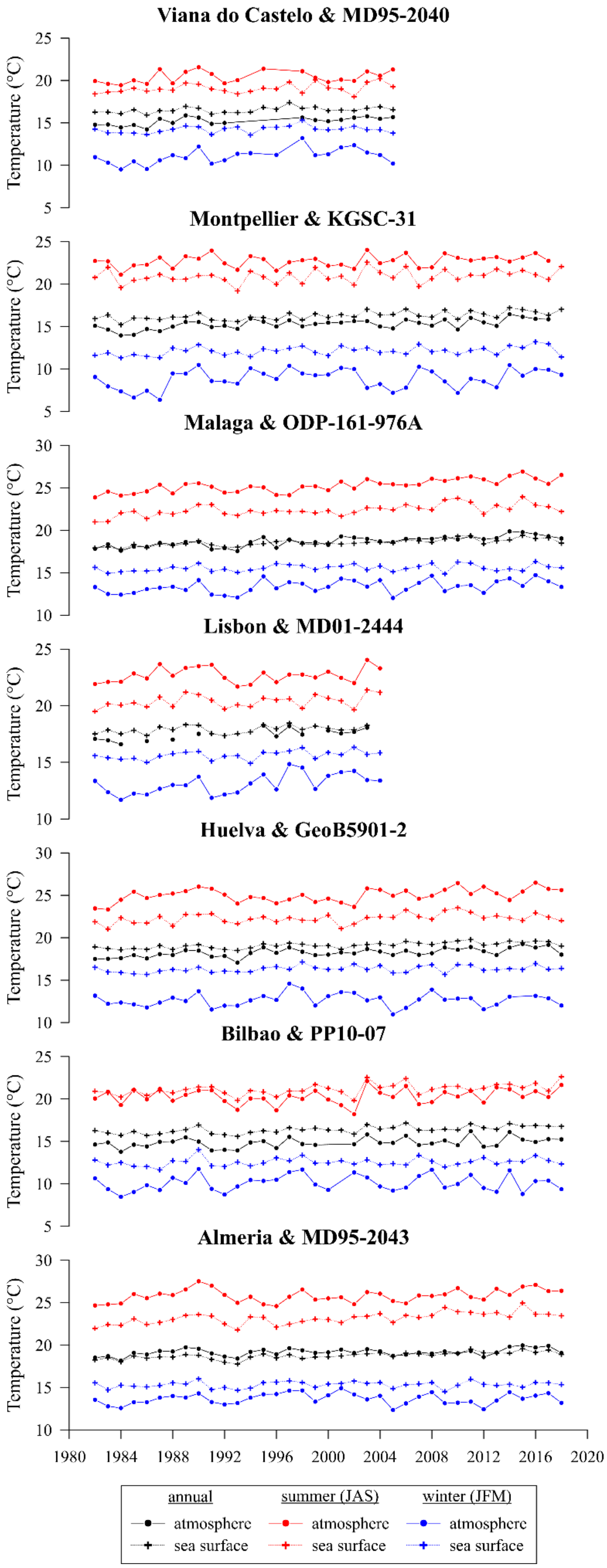

Fig. S2. Averaged seasonal (winter and summer) and annual sea surface temperatures from chosen locations of marine sedimentary archives as well as the according air temperatures from the closest station on land. Sea surface temperature data were provided by NOAA OISST V2 High Resolution Dataset. Air temperatures have been collected from the Spanish State Meteorological Agency (AEMET) and European Climate Assessment & Dataset (ECAD).

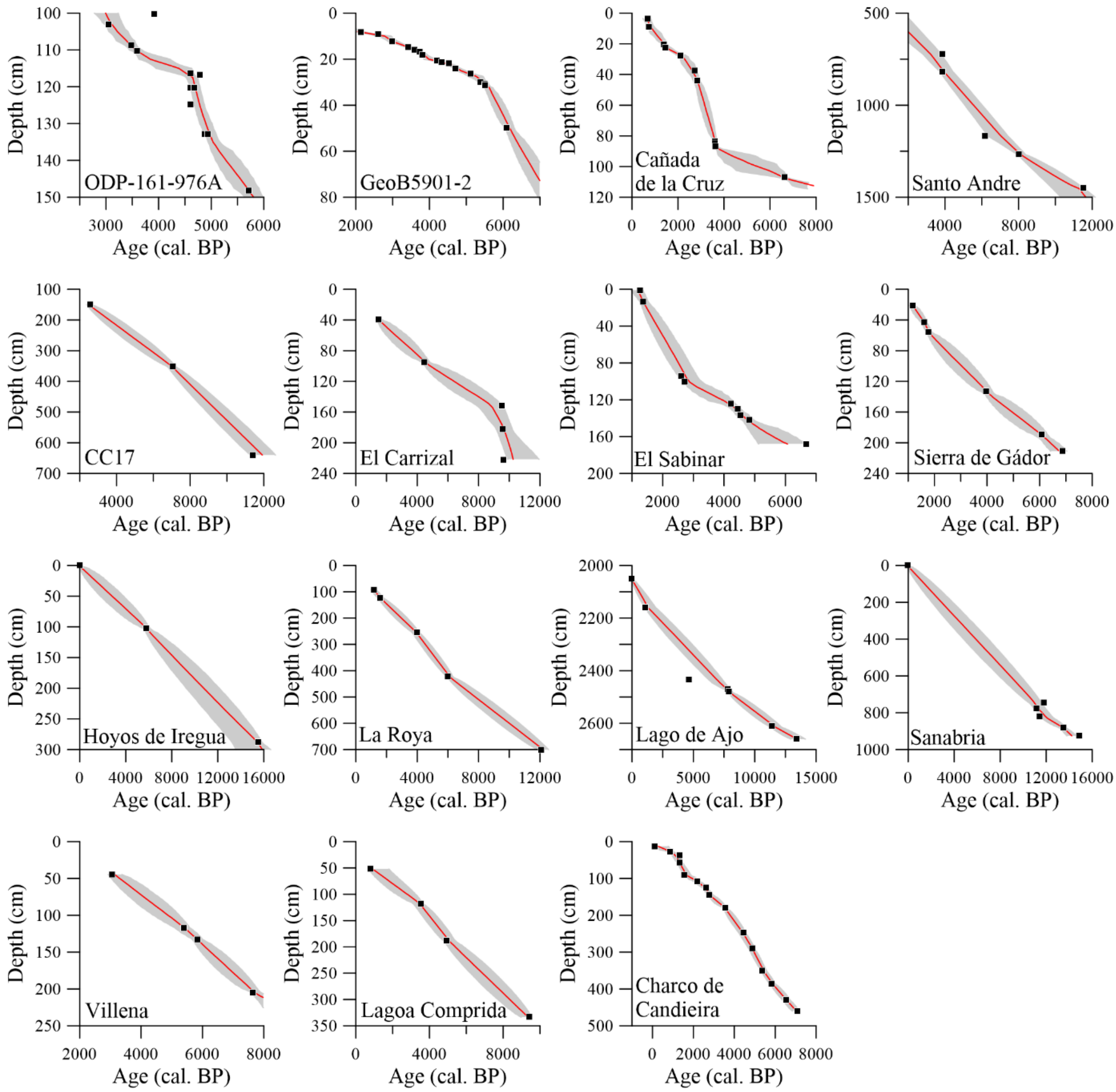

Fig. S3. Updated or calculated age models for all paleoclimatic archives. The source of the AMS ^{14}C data is referenced in Table 1 within the original publication.

Table S1. New AMS ^{14}C dates from sediment cores ODP-161-976A and GeoB5901-2.

Lab No.	depth (cm)	material	AMS ^{14}C age (yr BP)	error (yr)
ODP-161-976A				
KIA-54017	100.0 – 100.5	*G. ruber w+p*	3930	±40
KIA-54210	108.5 – 109.0	*G. ruber w+p*	3590	±35
KIA-54211	110.0 – 110.5	*G. ruber w+p*	3680	±30
KIA-54018	116.5 – 117.0	*G. ruber w+p*	4565	±35
KIA-54019	148.0 – 148.5	*G. ruber w+p*	5350	±55
GeoB5901-2				
KIA-54011	9.0 – 9.5	*G. ruber w+p*	2833	±26
KIA-54012	20.5 – 21.0	*G. ruber w+p*	4138	±29
KIA-54013	21.0 – 21.5	*G. ruber w+p*	4225	±28
KIA-54014	21.5 – 22.0	*G. ruber w+p*	4384	±28
KIA-54015	31.0 – 31.5	*G. ruber w+p*	5139	±29
KIA-54016	49.0 – 49.5	*G. ruber w+p*	5680	±35

References

Fick, S.E., Hijmans, R.J., 2017. WorldClim 2: New 1-km spatial resolution climate surfaces for global land areas. Int. J. Climatol. 37(12), 4302–4315. doi:10.1002/joc.5086.

Locarnini, R.A., Mishonov, A.V., Baranova, O.K., Boyer, T.P., Zweng, M.M., Garcia, H.E., Reagan, J.R., Seidov, D., Weathers, K., Paver, C.R., Smolyar, I., 2019. World Ocean Atlas 2018,: Volume 1: Temperature.